

BEHAVIOR OF LOW-FREQUENCY SOUND WAVES IN POROUS MEDIA

BY

TYLER JAMES ROSSI

THESIS

Submitted in partial fulfillment of the requirements
for the degree of Master of Science in Electrical and Computer Engineering
in the Graduate College of the
University of Illinois at Urbana-Champaign, 2010

Urbana, Illinois

Adviser:

Professor George W. Swenson, Jr.

ABSTRACT

This is a study of the relationship between the measured acoustic parameters and the measured physical parameters of porous media. Materials studied include crushed limestone, stream-formed pea gravel, large and small sifted pea gravels, and glass spheres. A standing wave curve fitting algorithm was applied to data taken from a vertical impedance tube to determine the propagation and reflection parameters of the materials. Physical characteristics considered include porosity, tortuosity, and flow resistivity.

ACKNOWLEDGMENTS

I would like to thank Dr. George Swenson, Jr. and Dr. Michael White for the support and advice they offered. The experiments performed throughout this project could not have been done without the technical expertise of Jeff Mifflin and Rob Kline. I would also like to thank Todd Borrowman for the continued assistance he gave me, particularly that concerning MATLAB programming. The experimental facilities described in this report were provided by the US Army Construction Engineering Research Laboratory under CESU agreement W9132T-09-2-0008-P00002.

TABLE OF CONTENTS

LIST OF FIGURES.....	v
LIST OF TABLES.....	vi
CHAPTER 1: INTRODUCTION.....	1
CHAPTER 2: TRANSMISSION LINE THEORY.....	3
CHAPTER 3: ACOUSTIC PARAMETER MEASUREMENT.....	7
CHAPTER 4: NON-ACOUSTIC PARAMETER MEASUREMENT.....	21
CHAPTER 5: RESULTS AND CONCLUSIONS.....	30
REFERENCES.....	33
APPENDIX A: IMPEDANCE TUBE DATA.....	34
APPENDIX B: EXPERIMENTAL TORTUOSITY DATA.....	41
APPENDIX C: EXPERIMENTAL FLOW RESISTIVITY DATA.....	45
APPENDIX D: MATLAB SOURCE CODE.....	49

LIST OF FIGURES

Figure 2.1: Transmission line.	3
Figure 2.2: Impedance tube.	4
Figure 3.1: CERL impedance tube.	8
Figure 3.2: Impedance tube speaker.	9
Figure 3.3: Test bench.	9
Figure 3.4: Materials tested.	11
Figure 3.5: Crushed limestone attenuation coefficient and wavelength values	15
Figure 3.6: Non-sifted pea gravel attenuation coefficient and wavelength values	16
Figure 3.7: Large sifted pea gravel attenuation coefficient and wavelength values	17
Figure 3.8: 10 mm glass spheres attenuation and wavelength vs. frequency	19
Figure 3.9: Attenuation coefficient vs. frequency.	20
Figure 3.10: Wavelength vs. frequency.	20
Figure 4.1: Tortuosity test apparatus.	23
Figure 4.2: Flow resistivity test apparatus.	26
Figure 4.3: Crushed limestone flow resistivity result.	27
Figure 4.4: Non-sifted pea gravel flow resistivity result.	28
Figure 4.5: Large sifted pea gravel flow resistivity result.	29
Figure 4.6: 10 mm glass spheres flow resistivity result.	29
Figure 5.1: Sphere packing vs. cell radius.	31

LIST OF TABLES

Table 3.1: Test Material Sieve Analysis.	10
Table 3.2: Crushed Limestone Acoustic Parameters.	15
Table 3.3: Non-Sifted Pea Gravel Acoustic Parameters.	16
Table 3.4: Large Sifted Pea Gravel Acoustic Parameters.	17
Table 3.5: Small Sifted Pea Gravel Acoustic Parameters.	18
Table 3.6: 10 mm Glass Spheres Acoustic Parameters.	19
Table 4.1: Porosity Results.	21
Table 4.2: Non-Sifted Pea Gravel Tortuosity Results.	24
Table 4.3: Large Sifted Pea Gravel Tortuosity Results.	24
Table 4.4: 10 mm Glass Spheres Tortuosity Results	25
Table 5.1: Attenuation Coefficient and Flow Resistivity Comparison.	30

CHAPTER 1

Introduction

Military training exercises consistently cause unwanted levels of noise pollution in the public areas surrounding test sites. For example, artillery and high-explosives detonations create high sound pressure waves that are able to travel long distances because most of the energy is located in the low-frequency region of 25-250 Hz characterized by low attenuation in air.

In an effort to develop methods to decrease the amount of sound pollution generated by military testing and training, researchers have looked at the possibility of using porous media to attenuate low-frequency sound waves. Early experimentation in this area began with field analysis such as detonating explosives at one end of a bed of gravel and taking measurements at the other end. This method was ultimately deemed unusable because atmospheric conditions and other parameters in the field were not controllable. To avoid such sources of error, the U.S. Army Corps of Engineers Engineer Resource Development Center / Construction Engineering Research Laboratory (ERDC/CERL) acoustics team constructed a low-frequency test chamber so that data could be collected in a laboratory setting.

The final design for the test chamber was a vertical, circular waveguide that could be filled to a certain depth with the porous material under test. The waveguide has drilled microphone ports at 20 cm intervals along the vertical axis and has both solid and mesh terminating plates that can be interchanged depending on the needs of the experiment. All data shown in this report were taken using this impedance tube. Materials tested include fine sand, coarse crushed limestone, pea gravel of various grades, and 10 mm diameter glass spheres.

Previous work at ERDC/CERL has provided methods for using the impedance tube to calculate the acoustic parameters of porous media [1], [2]. This thesis presents data on the

acoustical performance of additional materials not evaluated in the previous studies. Further, this thesis evaluates the materials' physical properties such as porosity, tortuosity, and flow resistivity in an effort to find a correlation to the acoustic properties. Discovering such a relationship would be valuable because it would allow one to determine the material best suited for an application without directly measuring the acoustic properties. There are several advantages to being able to test physical properties rather than acoustic properties. First, the experimental setup for an acoustic measurement is large and complicated, and requires expensive, well-calibrated equipment as well as a controlled environment. Additionally, the physical measurements generally require a much smaller material sample and can be completed much more quickly.

CHAPTER 2

Transmission Line Theory

In this chapter, electrical transmission line theory is introduced for the purpose of describing the behavior of sound waves within an acoustical impedance tube. It was natural to begin with the analog analysis of a transmission line rather than an acoustical duct because the people contributing to this project are electrical engineers and are therefore more familiar with the differential equations associated with the electrical transmission line and the corresponding impedance relations.

The following understanding of transmission line theory and its application to acoustical ducts arises from the discussions in [3], [4]. Consider the lossy transmission line shown in Figure 2.1.

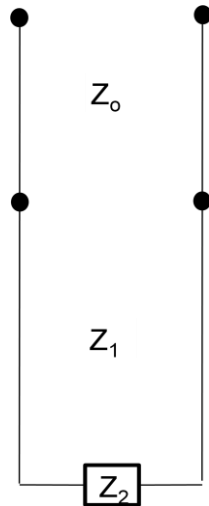


Figure 2.1: Transmission line.

Within the transmission line, a single-frequency plane wave travels away from the source at the upper termination. As the wave travels through the line and is incident on the load, a reflected wave of some magnitude is sent back up through the tube. In an electrical transmission line, the voltage a distance x away from the source is given by

$$V(x) = V^+ e^{x(\alpha + j\beta)} + V^+ \Gamma e^{-x(\alpha + j\beta)} \quad (2.1)$$

In an acoustical duct, the total pressure a distance x away from the source is given by

$$p(x) = A^+ e^{x(\alpha+j\beta)} + A^+ \Gamma e^{-x(\alpha+j\beta)} \quad (2.2)$$

The total voltage in Equation (2.1) and the total pressure in Equation (2.2) are described as the superposition of two waves. The first term represents the wave moving down the transmission line away from the source and the second term represents the wave that has reflected off the interface and is moving back up the transmission line toward the source. In Equation (2.2), A represents the complex root mean square pressure of the plane wave that is incident at the a-b interface from material a, $\Gamma = |\Gamma|e^{j\theta}$ represents the complex reflection coefficient of the a-b interface, α represents the attenuation coefficient, and β represents the phase constant.

Applying a sinusoidal input in Equation (2.2) gives

$$p(x)^2 = |A|^2 [1 + |\Gamma|^2 + 2|\Gamma| \cos\{2(\alpha + j\beta)x + \theta\}] \quad (2.3)$$

or

$$|p(x)| = A \sqrt{1 + |\Gamma|^2 + 2|\Gamma| \cos\{2(\alpha + j\beta)x + \theta\}} \quad (2.4)$$

Now consider the impedance tube shown in Figure 2.2, which contains both lossless and lossy regions. For the purposes of applying Equation (2.2), this impedance tube may be thought of as a three-layer system composed of a lossless region (medium 0), a lossy region (medium 1) located between $x = 0$ and $x = L$, and a hard-reflecting termination (medium 2) located at $x \leq 0$.

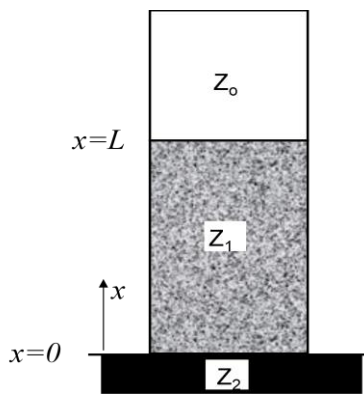


Figure 2.2: Impedance tube.

In medium 0, $\alpha_0 = 0, c = 343 \frac{m}{s}, \beta_0 = \frac{2\pi f}{c}$. The corresponding parameters associated with medium 1 are unknown and must be evaluated experimentally. Further, all energy incident on the hard-reflecting surface at $x = 0$ is reflected back, giving $\Gamma_{12} = 1$. Applying Equation (2.2) to this system gives

$$p(x, f) = \begin{cases} A_0(e^{j\beta_0(x-L)} + \Gamma_{01}e^{-j\beta_0(x-L)}), & x \geq L \\ A_1(e^{x[\alpha_1(f) + j\beta_1(f)]} + e^{-x[\alpha_1(f) + j\beta_1(f)]}), & L \geq x \geq 0 \end{cases} \quad (2.5)$$

In the lossy region between $x = 0$ and $x = L$, the downward-traveling wave is exponentially attenuated as it travels toward $x = 0$, and the upward traveling wave is exponentially attenuated as it travels away from $x = 0$. In the lossless region above $x = L$, a standing wave exists with a standing wave ratio given by

$$SWR = \frac{1 + |\Gamma_{01}|}{1 - |\Gamma_{01}|} \quad (2.6)$$

The input impedance looking into the layer of porous media is then given by

$$Z_L = Z_0 \frac{1 + \Gamma_{01}}{1 - \Gamma_{01}} \quad (2.7)$$

where Z_0 is the characteristic impedance of air, here taken as a real number, approximately $413 \text{ Pa} \cdot \text{s/m}$.

To characterize the waves traveling through the impedance tube fully, $\alpha_1(f), \beta_1(f), A_0, A_1$, and Γ_{01} must be determined through experimentation. It is worth noting that the phase constant, β , may be calculated by determining either the phase velocity or the wavelength, as shown in Equation (2.8).

$$\beta_1 = \frac{2\pi f}{v_1(f)} = \frac{2\pi}{\lambda_1} \quad (2.8)$$

This introduces some freedom to investigate the phase constant through multiple methods and compare the results.

In order to accurately measure the pressure within the impedance tube, it is necessary to ensure that no transverse modes are propagating. The presence of transverse modes operating within the tube would create pressure fluctuations and introduce error to the calculations. Since the frequency range of interest is 25-250 Hz, it is necessary to construct an impedance tube with dimensions that do not support transverse modes below 250 Hz.

The cutoff frequency for the dominant transverse mode in a cylindrical cavity is given by

$$\omega < 1.841 \frac{c}{a} \quad (2.9)$$

where a represents the cross-section radius [3]. Below this frequency, the transverse waves are evanescent and cannot propagate. Using $c = 330 \frac{\text{m}}{\text{s}}$ as the worst-case air speed and $f = 250 \text{ Hz}$ for the upper frequency boundary gives

$$a < 1.841 \frac{330}{500\pi} = 38.65 \text{ cm} \quad (2.10)$$

The relation in Equation (2.10) creates a restriction on the dimensions of the impedance tube used in experimentation.

CHAPTER 3

Acoustic Parameter Measurement

3.1 Facilities

Early attempts to study the acoustic properties of different materials such as vegetation used a horizontal impedance tube to measure the pressures of a standing wave when the chamber was filled with different materials [5]. This method was found to be inadequate for experiments with non-rigid media. With such materials, a vertical arrangement allows for a more homogenous distribution of the material inside the chamber. Therefore the ERDC/CERL acoustics team designed a vertical impedance tube for experimenting with porous media in the low-frequency range.

The impedance tube is 7.25 m long and constructed from Schedule 80 steel pipe with a diameter of 76 cm. This geometry is important in that the tube resonates at approximately 25 Hz and no transverse modes are excited at frequencies below 250 Hz. At full capacity the impedance tube holds just over 3 m³ of the test material.

Along the vertical (propagation) axis, 36 ports are drilled at 20 cm intervals with the bottom-most port drilled vertically through the bottom termination. These holes serve as probe points that accept either 1 in microphones or ½ in microphones held in a Teflon adaptor. A rubber gasket creates an air-tight seal around the microphone in each port. A wire mesh covers each port on the inside of the tube to prevent the test material from entering the microphone ports. A steel plug seals each port not in use during experimentation.

The top termination of the tube holds a 12 in speaker that serves as the sound source during experimentation. The speaker is rigged in a plywood mount and bolted to the top opening of the tube. The speaker is driven either by a function generator producing a single-frequency

tone or by a random noise generator band-limited from 20-200 Hz. The bottom termination of the tube is a steel plate that has been bolted on. This plate serves as a pressure-doubling surface with a reflection coefficient between 0.94 and 1.00 at test frequencies [1].

Of the 36 available ports, data can be simultaneously recorded from 32 ports using two Yokogawa model DL750 oscilloscopes slaved to a trigger switch. The reference-grade microphones used for data collection are Larson Davis Laboratories model 2540 and Brüel & Kjær models 4144, 4145, 4190, 4191, and 4193.

The figures below show the test apparatus used to measure acoustic parameters. Figure 3.1 shows the erect impedance tube without microphones. Figure 3.2 shows the 12 in speaker mounted to the top of the impedance tube. Figure 3.3 shows the test bench, complete with oscilloscopes, a signal generator, a band pass filter, and an amplifier.



Figure 3.1: CERL impedance tube (left) with close-up of microphone ports (right).



Figure 3.2: 12 in speaker set in the top of the impedance tube. Courtesy of Tim Eggerding.



Figure 3.3: Test bench for gathering pressure data.

3.2 Materials Studied

Several types of porous media have been tested in the impedance tube. Testing began with CA-7 crushed limestone and stream-formed pea gravel [1], [2]. The crushed limestone gravel originated from Kankakee, IL and consists of pure limestone. It has a large particle size and a wide range of particle sizes and shapes. The pea gravel samples feature smaller, more-

uniform particles. A sifting device was then used to create a sample set containing only particles with diameter less than 11 mm and a sample set containing only particles with diameter greater than 11 mm. These sifted pea gravel samples were also tested in the impedance tube to investigate how the acoustic parameters relate to particle size. Finally, 10 mm glass spheres were tested to evaluate a sample with uniform particle size and shape. Detailed particle size analysis and images of the samples are given in Table 3.1 and Figure 3.4. Particle size analysis was performed according to standard practices (USACE 1970 and ASTM 2007).

Table 3.1: Test Material Sieve Analysis

Crushed Limestone	
Grain Size (mm)	% of Particles
< 25	100
< 12.5	50
< 6.3	7.5
< 1.8	2

Non-Sifted Pea Gravel	
Grain Size (mm)	% of Particles
< 12.5	100
< 6.3	35
< 1.8	7

Large Sifted Pea Gravel	
Grain Size (mm)	% of Particles
< 12.5	100
< 11	0

Small Sifted Pea Gravel	
Grain Size (mm)	% of Particles
< 11	100
< 4	0

10 mm Glass Spheres	
Grain Size (mm)	% of Particles
10	100

Since the acoustic tests are conducted at a very low frequency range, the operating wavelength is much greater than particle sizes and the mechanical parameters are homogeneous on the scale of a few particle diameters.

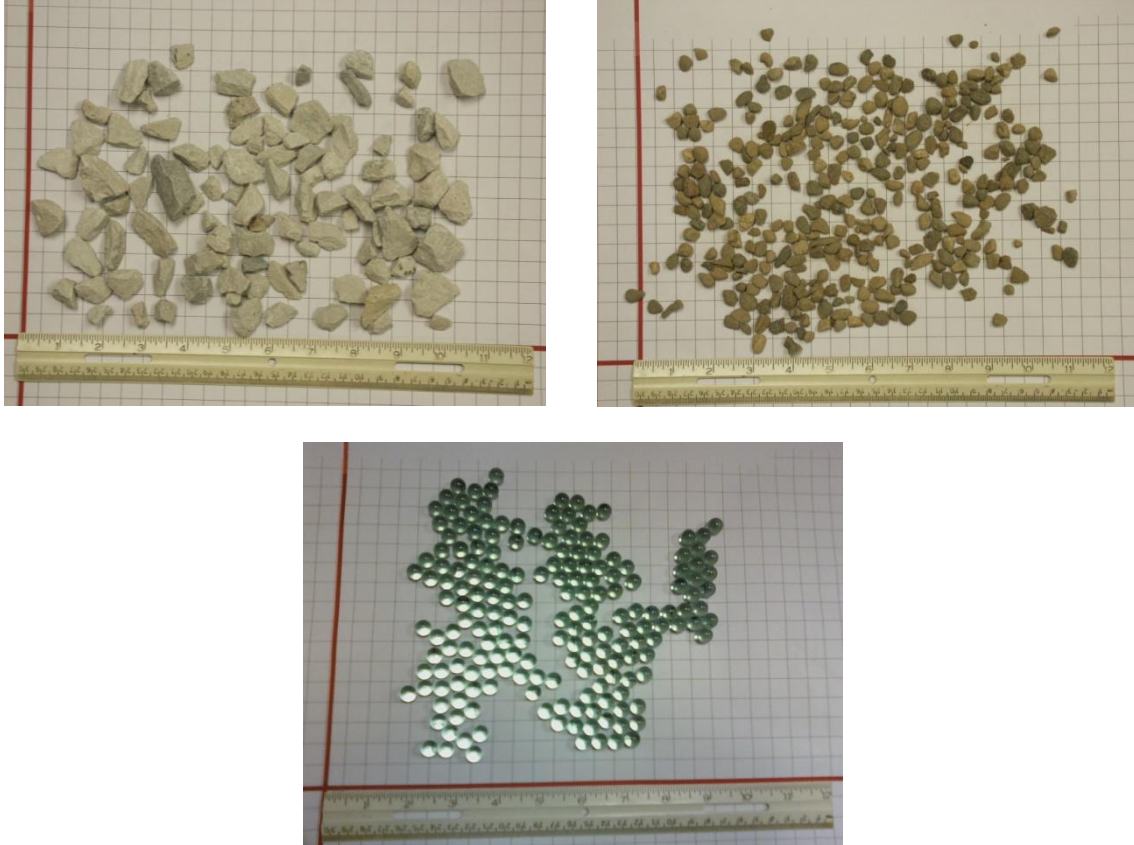


Figure 3.4 Materials tested: crushed limestone (left), pea gravel (right), glass spheres (bottom).

3.3 Acoustic Tests

Experimental procedures were identical for all materials investigated. The impedance tube was filled to progressively higher levels with the porous material. A crane was used to drop material through the speaker opening while the impedance tube stood on end, fastened securely to the floor and a supporting column. This was typically done in 1 m increments until material supplies were exhausted. Microphones were arranged in the ports such that all the channels in the filled region of the tube were used as well as several channels in the air region. Prior to taking data, all microphones being used were calibrated using a Brüel & Kjær model 4228 piston phone. Data was recorded for discrete frequencies of 25, 50, 75, 100, 120, 150, 170, and 200 Hz. Noise samples band-limited between 20 Hz and 200 Hz were also recorded. Multiple sets of data were generally taken for each level of material in the tube for redundancy.

3.4 Standing Wave Curve Fitting

Filling the impedance tube to a known depth with some porous medium and measuring the sound pressure throughout the tube allows one to evaluate the attenuation and phase velocity parameters within the test material as well as the reflection characteristics at the boundary.

When the sound wave travels down from the speaker and reaches the air-material interface, part of the energy is reflected back toward the top. The rest of the energy is transmitted through the interface, is attenuated as it passes through the material, and then reflects off the termination. As discussed in Chapter 2, this system is a duct with two sections of different acoustical parameters. Therefore, the acoustic parameters must be evaluated separately in each region.

The air region of the impedance tube is considered lossless and acts as a lossless transmission line. Therefore, Equation (2.3) is applied to the air region of the tube using a minimum mean-square error (MMSE) method to solve for the unknown parameters. Initial values are chosen for the parameters A_0 , $|\Gamma_{01}|$, and θ_{01} to calculate a pressure value $p_{n,estimate}$ that is compared with the measured pressure value. The value for $|\Gamma_{01}|$ is then stepped through the range $[0,1]$ and the value for θ_{01} is stepped through the range $[0,2\pi]$, while the range for A_0 is determined by the experimental values. For each set of estimated parameter values, the mean-square error (MSE) is calculated by

$$MSE = \frac{1}{N} \sum_{n=1}^N [p_{n,measured}(n) - p_{n,estimate}(n)]^2 \quad (3.1)$$

and the set of parameter values that minimizes the MSE is chosen as the best estimate. Since the parameters are frequency-dependent, this process must be completed for each frequency tested as well as for each level of test material placed in the tube. Once the best estimates for A_0 , $|\Gamma_{01}|$, and θ_{01} have been determined, the standing wave ratio (SWR) and input impedance can be calculated from Equations (2.5) and (2.6). These calculated parameter values for given test

material and material depth are given in Tables 3.2 through 3.6. Some of the data for crushed limestone and pea gravel were taken from [1] and [2]. The raw data gathered from the impedance tube are presented in Appendix A. The MATLAB code used for MMSE fitting is presented in Appendix D.

The reflective properties discussed above do not fully describe the materials under test. The propagation characteristics of the material are also of interest. A volume of porous media is composed of some combination of particles and empty space that is not necessarily homogeneous. Sound energy traveling through a volume of porous material may reflect off individual particles, transmit through particles, or pass through the empty space between particles. Therefore, the part of the impedance tube containing test material is equivalent to a lossy transmission line. The parameters within the porous medium are different from those in air, and must be estimated separately. In this case, the condition $\Gamma_{12} = 1e^{j0}$ is used since the terminating boundary has been shown to approximate a perfect reflector. However, the values of the propagation constants α_1 and β_1 are unknown and must be estimated via the MMSE method along with A_1 . The β_1 values are calculated from Equation (2.7). The calculated parameter values for given test material and material depth are given in Section 3.5.

3.5 Results

Tables 3.2 through 3.6 display the calculated acoustic reflection parameters for all materials tested. In these tables, $|\Gamma|$ represents the absolute value of the reflection coefficient at the material boundary; Θ represents the phase angle of this reflection coefficient in radians; SWR represents the standing wave ratio as described in Equation (2.6), and Z_L/Z_0 represents the ratio of the load impedance seen from the air region to the characteristic acoustic impedance in air. Tables 3.2 through 3.6 also display propagation parameters within the media. The attenuation coefficient is represented by α with units of Np/m. The wavelength at which the sound waves are traveling within the media is represented by λ in meters. The phase constant of the traveling wave is represented by β in rad/m. The phase velocity is represented by v in m/s. The data used to construct Table 3.2 can be found in [1]. The data used to construct Table 3.3 can be found in [2] and was compiled using a max correlation method described therein. The data used to construct Tables 3.4 through 3.6 can be found in Appendix A of this thesis. Figures 3.5 through 3.8 plot the experimental values for α and λ for the frequencies considered.

Table 3.2: Crushed Limestone Acoustic Parameters

1 meter					2 meters			
Freq	$ \Gamma $	Θ	SWR	Z_L/Z_0	$ \Gamma $	Θ	SWR	Z_L/Z_0
25	0.84	6.28	11.5	11.50+0.0j	0.47	4.65	2.77	0.61-0.73j
50	0.26	5.28	1.70	1.18-0.56j	0.73	3.58	6.41	0.16-0.22j
75	0.66	4.34	4.88	0.29-0.64j	0.52	2.20	3.17	0.39+0.44j
100	0.75	4.08	7.00	0.18-0.50j	0.67	0.50	5.06	2.01+2.35j
150	0.54	3.14	3.35	0.30+0.0j	0.58	3.83	3.60	0.30-0.33j
200	-	-	-	-	0.54	0.94	3.35	1.08+1.33j

3 meters					4 meters			
Freq	$ \Gamma $	Θ	SWR	Z_L/Z_0	$ \Gamma $	Θ	SWR	Z_L/Z_0
25	0.69	4.15	5.45	0.24-0.53j	0.43	3.20	2.51	0.40-0.03j
50	0.59	1.70	3.88	0.44+0.78j	0.49	5.22	2.92	0.99-1.12j
75	0.59	5.65	3.88	1.66-1.76j	0.60	1.57	4.00	0.47+0.88j
100	0.60	3.33	4.00	0.25-0.86j	0.60	4.40	4.00	0.37-0.66j
150	0.65	4.65	4.71	0.38-0.86j	0.51	3.46	3.08	0.33-0.14j
200	0.56	6.22	3.55	3.51-0.36j	0.50	2.58	3.00	0.36+0.26j

6.8 meters				
Freq	α	λ	β	ν
25	0.20	6.16	1.0200	154
50	0.28	3.32	1.8925	166
75	0.32	2.24	2.8050	168
100	0.38	1.69	3.7179	169
150	0.45	1.06	5.9275	159
200	0.53	0.75	8.3776	150

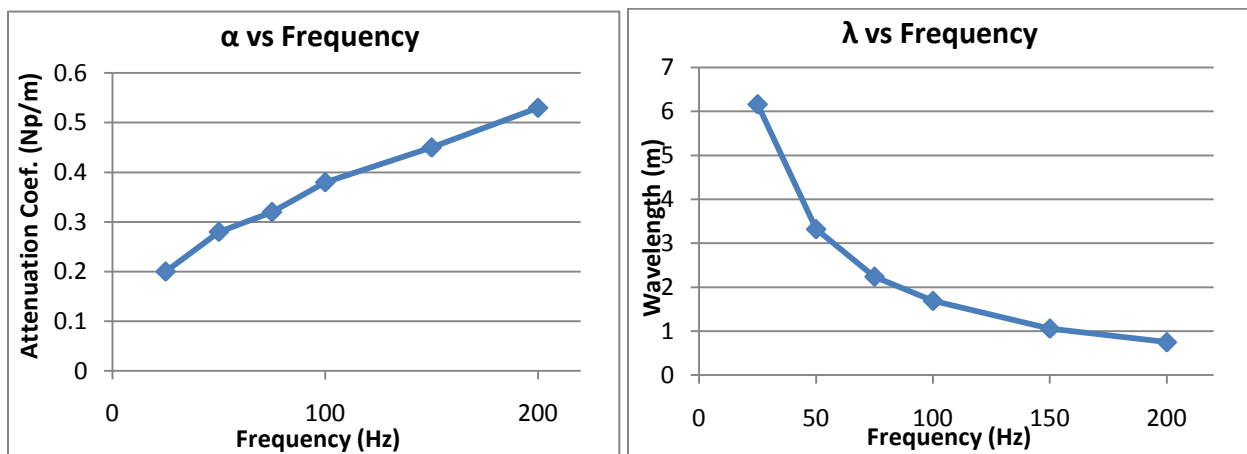


Figure 3.5: Crushed limestone attenuation coefficient and wavelength values.

Table 3.3: Non-Sifted Pea Gravel Acoustic Parameters

1 meter					2 meters			
Freq	$ \Gamma $	Θ	SWR	Z_L/Z_0	$ \Gamma $	Θ	SWR	Z_L/Z_0
25	0.79	0.062	8.52	7.96+2.1j	0.59	5.15	3.88	0.771-1.26j
50	0.58	6.16	3.76	3.58-0.784j	0.7	3.9	5.67	0.203-0.382j
75	0.57	5.34	3.65	1.03-1.41j	0.59	2.58	3.88	0.278+0.27j
100	0.71	5.15	5.9	0.551-1.43j	0.63	1.63	4.41	0.409+0.852j
150	0.71	4.71	5.9	0.33-0.944j	0.66	5.28	4.88	0.775-1.53j
200	0.54	3.83	3.35	0.334-0.324j	0.66	2.83	4.88	0.21+0.152j

3 meters					4 meters			
Freq	$ \Gamma $	Θ	SWR	Z_L/Z_0	$ \Gamma $	Θ	SWR	Z_L/Z_0
25	0.76	4.08	7.33	0.171-0.498j	0.73	3.14	6.41	0.156-0.0j
50	0.66	1.70	4.88	0.353+0.818j	0.63	5.91	4.41	2.68-2.06j
75	0.61	5.65	4.13	1.63-1.86j	0.59	2.45	3.88	0.289+0.33j
100	0.62	3.52	4.26	0.243-0.18j	0.63	5.59	4.41	1.42-1.89j
150	0.5	5.09	3.00	0.85-1.05j	0.67	5.22	5.06	0.696-1.46j
200	0.43	6.22	2.51	2.50-0.165j	0.68	4.71	5.25	0.368-0.93j

7 meters				
Freq	α	λ	β	ν
25	0.398	6.36	0.988	159.0
50	0.550	3.61	1.739	180.6
75	0.644	2.62	2.491	189.2
100	0.728	1.93	3.252	195.1
150	0.908	1.32	4.727	200.8
200	1.09	1.01	6.217	202.9

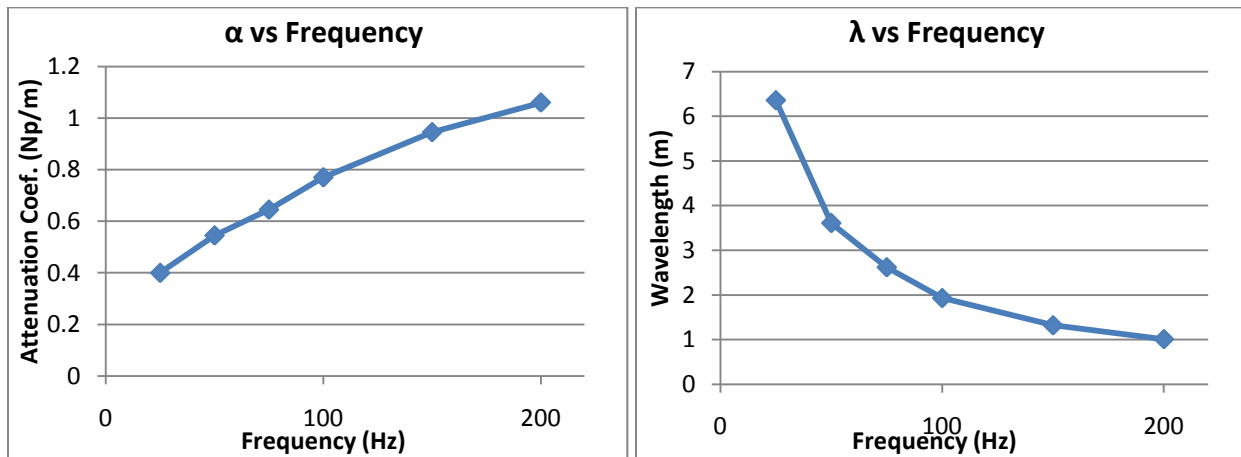


Figure 3.6: Non-sifted pea gravel attenuation coefficient and wavelength values.

Table 3.4: Large Sifted Pea Gravel Acoustic Parameters

1 meter					2 meters			
Freq	$ \Gamma $	Θ	SWR	Z_L/Z_0	$ \Gamma $	Θ	SWR	Z_L/Z_0
25	0.81	5.78	9.53	1.45-3.30j	0.63	0.628	4.41	1.6+1.96j
50	0.70	4.90	5.67	0.415-1.12j	0.55	0.88	3.44	1.16+1.41j
75	0.55	4.78	3.44	0.565-0.89j	0.51	1.32	3.08	0.735+0.982j
100	0.71	4.08	5.90	0.212-0.491j	0.54	2.01	3.35	0.404+0.558j
150	0.60	3.08	4.00	0.25+0.029j	0.51	2.83	3.08	0.332+0.141j
170	0.63	2.01	4.41	0.312+0.59j	0.48	3.71	2.85	0.337-0.252j

4 meters

Freq	$ \Gamma $	Θ	SWR	Z_L/Z_0
25	0.47	5.97	2.77	2.38-0.889j
50	0.69	6.28	5.45	5.45-0.0j
75	0.66	0.063	4.88	4.77+0.701j
100	0.63	6.28	4.41	4.41-0.0j
120	0.62	6.22	4.26	4.19-0.53j
150	0.62	6.22	4.26	4.19-0.53j
170	0.63	6.28	4.41	4.41-0.0j
200	0.55	0.126	3.44	3.3+0.653j

4 meters

Freq	α	λ	β	ν
25	0.40	9.00	0.6981	225
50	0.51	4.60	1.3659	230
75	0.57	2.90	2.1666	217
100	0.60	2.23	2.8176	223
120	0.65	1.84	3.4148	220
150	0.73	1.49	4.2169	223
170	0.73	1.41	4.4562	239
200	0.80	1.20	5.2360	240

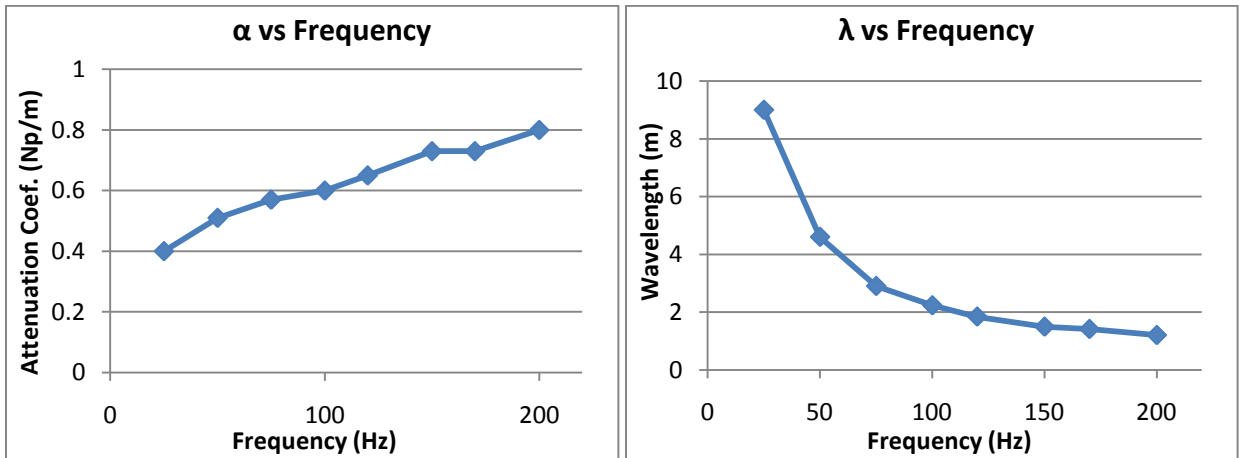


Figure 3.7: Large sifted pea gravel attenuation coefficient and wavelength values.

Table 3.5: Small Sifted Pea Gravel Acoustic Parameters

2 meters				
Freq	$ \Gamma $	Θ	SWR	Z_L/Z_0
25	0.74	5.22	6.69	.542-1.55j
50	0.74	4.02	6.69	0.182-0.458j
75	0.60	2.89	4.00	0.254+0.118j
100	0.47	1.95	2.77	0.497+0.558j
120	0.44	1.45	2.57	0.774+0.806j
150	0.53	5.97	3.26	2.64-1.20j
170	0.46	3.96	2.70	0.428-0.364j
200	0.37	4.59	2.17	0.702-0.597j

Table 3.5 displays the small sifted pea gravel results from standing-wave curve fitting in the air region. For this material, standing-wave curve fitting could not be applied to the filled region of the impedance tube because so little of the small gravel was available. After the sifting process, approximately 2 m of small gravel was available for experimentation, which provided very few data points in the impedance tube.

Table 3.6 10 mm Glass Spheres Acoustic Parameters

1 meter					1.8 meters			
Freq	$ \Gamma $	Θ	SWR	Z_L/Z_0	$ \Gamma $	Θ	SWR	Z_L/Z_0
25	0.85	5.84	12.3	1.51-3.93j	0.68	5.4	5.06	0.93-1.74j
50	0.58	5.28	3.76	0.93-1.37j	0.63	0.628	4.41	1.60+1.96j
75	0.30	1.19	1.86	1.05+0.64j	0.75	6.28	7.00	7.00+0.00j
100	0.71	0.44	5.9	2.26+2.76j	0.49	5.65	2.92	1.70-1.29j
120	0.83	0.126	10.8	7.41+4.95j	0.50	0.628	3.00	1.70+1.33j
150	0.81	6.03	9.53	3.95-4.63j	0.72	6.28	6.14	6.14-0.00j
170	0.71	5.72	5.9	1.63-2.49j	0.58	5.84	3.76	2.31-1.72j
200	0.15	5.65	1.35	1.25-0.23j	0.51	0.628	3.08	1.70+j1.38

3 meters					3.8 meters			
Freq	$ \Gamma $	Θ	SWR	Z_L/Z_0	$ \Gamma $	Θ	SWR	Z_L/Z_0
25	0.44	0.377	2.57	2.15+0.863j	1.00	0.251	inf	0.00+7.92j
50	0.71	5.91	5.9	2.7-2.84j	0.37	6.16	2.17	2.14-0.23j
75	0.52	0.063	3.17	3.14+0.28j	0.61	5.97	4.13	2.96-1.78j
100	0.55	5.72	3.44	1.87+1.58j	0.67	6.16	5.06	4.61-1.41j
120	0.51	6.22	3.08	3.06-0.265j	0.51	6.09	3.08	2.87-0.74j
150	0.51	5.72	3.08	1.85-1.37j	0.53	5.91	3.28	2.43-1.32j
170	0.54	6.03	3.35	2.89-1.09j	0.57	5.91	3.65	2.55-1.58j
200	0.39	5.78	2.28	1.81-0.80j	0.57	5.97	3.65	2.80-1.46j

3.8 meters				
Freq	α	λ	β	ν
25	0.16	9.86	0.6372	246.5
50	0.19	5.06	1.2417	253
75	0.21	3.44	1.8265	258
100	0.25	2.57	2.4448	257
120	0.28	2.16	2.9089	259.2
150	0.30	1.75	3.5904	262.5
170	0.32	1.53	4.1067	260.1
200	0.35	1.32	4.7600	264

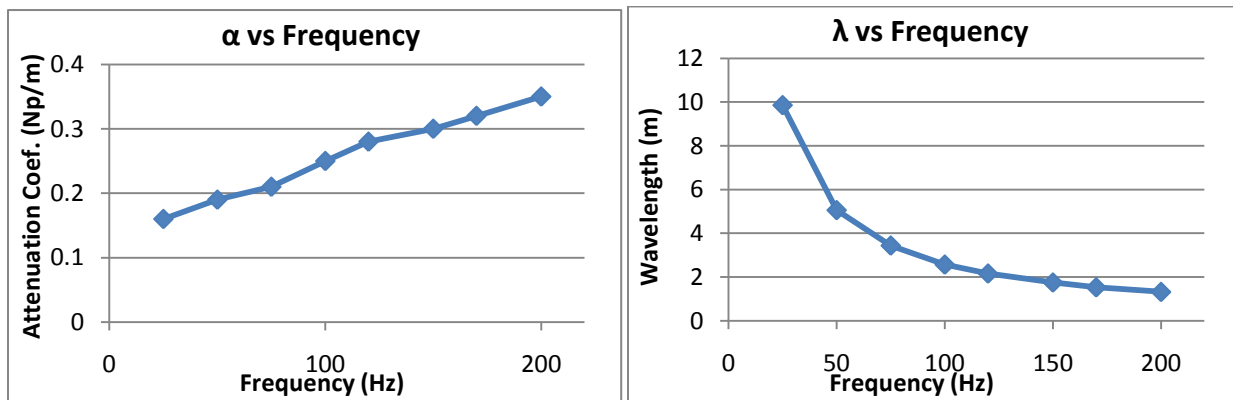


Figure 3.8: Attenuation coefficient and wavelength vs. frequency for glass spheres.

Comparison plots are shown in Figures 3.9 and 3.10 for four materials. Figure 3.9 compares the attenuation coefficients of the materials while Figure 3.10 compares the wavelength within the impedance tube. There was not enough small sifted pea gravel available to yield meaningful attenuation and wavelength values. Therefore, the small pea gravel data set is not included here. As shown in the plots, the pea gravel samples have the highest attenuation of the materials tested, followed by the limestone gravel and the glass spheres. The opposite appears true of the wavelength within the test materials

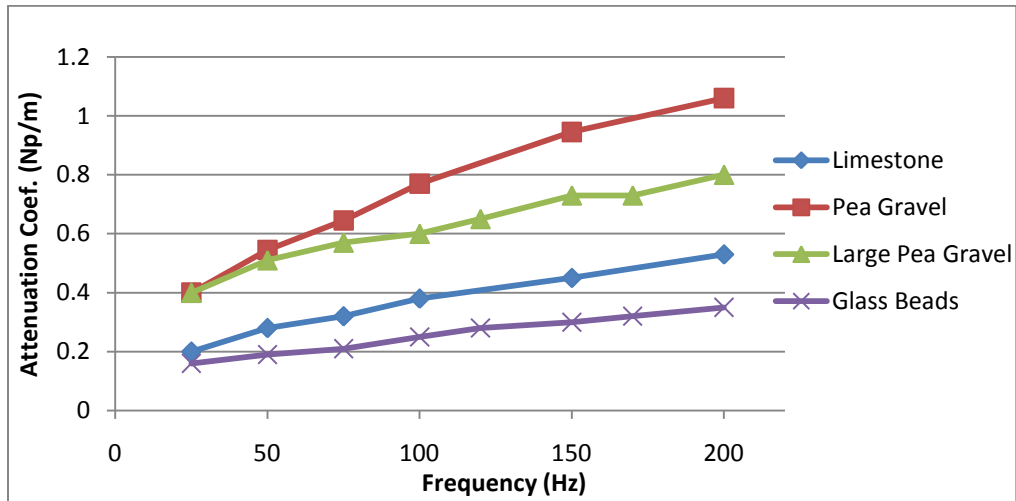


Figure 3.9: Attenuation coefficient vs. frequency.

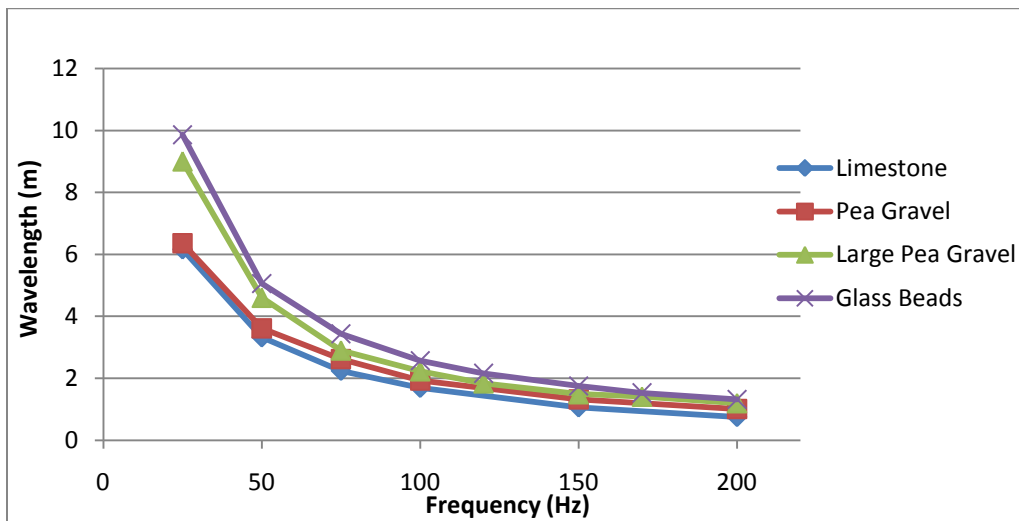


Figure 3.10: Wavelength vs. frequency.

CHAPTER 4

Non-Acoustic Parameter Measurement

4.1 Porosity

The porosity of a porous material is a measure of the void spaces in the material. It is calculated by taking the ratio of the volume of empty space between particles over the entire volume of the material. Therefore, the porosity values can range from 0-1 or from 0-100%. To experimentally calculate porosity, a container was filled with a known volume of water. Then the container was filled to the same level with test material. Water was poured over the test material until it reached the top of the material. This volume of water was compared to the volume of water used without the test material in order to determine the porosity. Table 4.1 summarizes the results for the porosity tests. Detailed data is given in Appendix B.1.

Table 4.1: Porosity Experimental Results

Material	Average Porosity Value
Non-Sifted Pea gravel	0.35
Large Sifted Pea Gravel	0.42
10 mm Glass Spheres	0.369

4.2 Tortuosity

Tortuosity is the ratio of the average path length a wavelet in air takes when it flows through a material to the average path length the wavelet takes without the material present. It would be difficult to measure tortuosity via air flow. However, Dr. George Swenson, Jr. at ERDC/CERL developed a method for indirectly measuring the tortuosity of a porous material using electrical current rather than air. When the material is saturated with a conducting fluid such as salt water, electricity follows the same path through the material that air would in the dry material. Assuming that the electrical resistivity of the liquid electrolyte is constant, the electrical resistance is proportional to the path length electric current takes. Therefore, the

tortuosity is related to the relative electrical resistance of the saturated media compared to the electrical resistance of the conducting liquid alone. One must note, however, that air does not only take the most direct path available. Instead, it will spread out if space is available. The measure of air space inside the material, its porosity, must be taken into account. The tortuosity is therefore calculated as porosity times the electrical resistance of the gravel saturated in a conducting fluid divided by the electrical resistance of the conducting fluid:

$$t = p * R(\text{gravel} + H_2O) / R(H_2O) \quad (4.1)$$

This derivation assumes that the liquid electrolyte does not saturate the material particles.

The experimental procedure used to measure the tortuosity of various samples is detailed in the steps below:

1. Construct a test cell such that two opposing faces are lined with a sheet of highly electrically conductive material. The remainder of the test chamber must be both non-conducting and water tight.
2. Fill the cell with the material under test. Measure the resistance R_m between the conducting faces to ensure that the material is not conductive.
3. Fill the cell containing material with a liquid electrolyte and measure the resistance R_s .
4. Empty the cell and refill with the same electrolyte. Measure the resistance R_e .
5. Assuming $R_s \ll R_m$, $R_s = R_e t / p$.
6. If the inequality in 5 does not hold, consider R_m in parallel with R_s .

The test apparatus used for the experiments detailed in this thesis is shown in Figure 4.1. It consists of a PVC tube 0.85 m tall and four inches in diameter. One of the conducting surfaces is a wire mesh located at the bottom of the tube. The top of the tube is left open and a stick with another metal mesh on the end can be inserted through the opening such that the second mesh rests on top of the material placed in the tube for testing. The two wire meshes then serve as the

electrodes across which the tube voltage is measured. A resistor with a known resistance is placed in series with the tube circuit in order to determine the current flowing through the tube. An input voltage of approximately 5 Vac was used. Alternating current was chosen due to problems using DC power in the past. It is presumed that DC current flowing through the electrolyte solution causes ions to travel to either side of the test chamber and coat the electrodes. Hydrogen ions coating the anode create an insulating layer that interferes with the experiment.

Several problems were encountered while testing material tortuosity. It is clear that the conductivity, and therefore the salinity of the electrolyte solution must be equal for both the measurement of the solution alone and the measurement of the solution with material. While it is easy to control the salinity of the solution used in the experiments, it is difficult to know how the moisture absorbed by individual particles or the salt residue on the particles will affect the results. Further, the gravel samples contained some amount of dust, which collected as mud in the bottom of the test chamber when the gravel was immersed in the salt solution. This mud clogged the pores between particles and effectively changed the characteristics of the material samples.

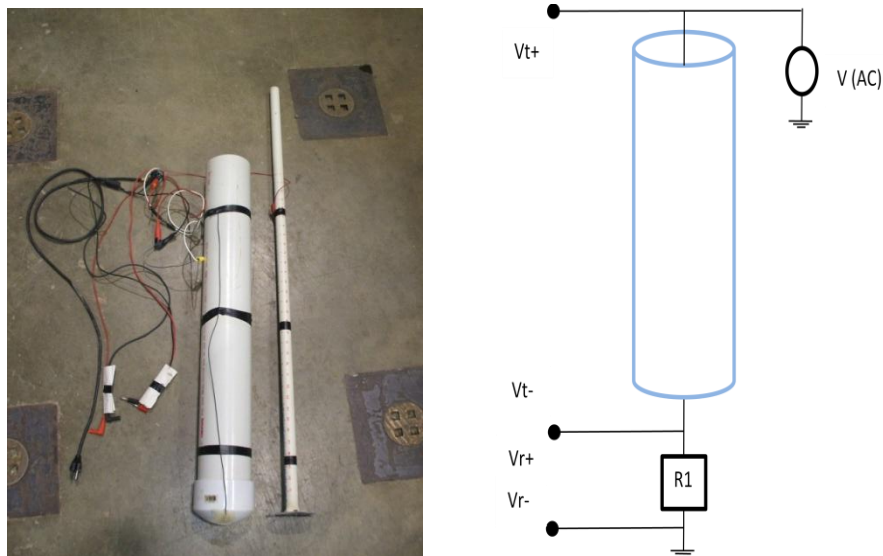


Figure 4.1: Tortuosity experiment equipment and circuit diagram.

4.2.1 Non-Sifted Pea Gravel

The tortuosity experiments using non-sifted pea gravel were performed previously at CERL by Erica Lynn in October 2007. A summary of the results is given in Table 4.2. The complete data are given in detail in Appendix B.1.

Table 4.2: Non-Sifted Pea Gravel Tortuosity

Trial #	Tortuosity
1	1.485
2	1.489
3	1.507
4	1.543
5	1.548
Average Tortuosity = 1.52	
Standard Deviation = 0.038	

4.2.2 Large Sifted Pea Gravel

The sifted pea gravel used in tortuosity evaluations produced very inconsistent results at first. This problem was resolved by washing the gravel sample after each trial and allowing it to dry thoroughly. Although this method made the process very time consuming, the tortuosity values converged well. A summary of the results is given in Table 4.3. The complete data are given in detail in Appendix B.2.

Table 4.3: Large Sifted Pea Gravel Tortuosity

Trial #	Tortuosity
1	1.76
2	1.64
3	1.72
4	1.88
5	1.66
Average Tortuosity = 1.732	
Standard Deviation = 0.0854	

4.2.3 10 mm Diameter Spheres

In general, the glass spheres gave consistent results between trials, presumably due to their lack of absorption or dust. The results of 5 tortuosity experiments using 10 mm glass spheres are summarized in Table 4.4. Complete experimental data may be found in Appendix B.3.

Table 4.4: 10 mm Glass Spheres Tortuosity

Trial #	Tortuosity
1	1.14
2	1.33
3	1.145
4	1.18
5	1.19
Average Tortuosity = 1.197	
Standard Deviation = 0.0693	

4.3 Flow Resistance

The static flow resistance of a porous material is calculated by taking the ratio of the pressure gradient across a material sample over the velocity of air flow through that sample. Graphing the pressure gradient divided by the flow velocity versus the flow velocity results in a plot where the y-intercept is the static flow resistivity. The slope of the plot then represents $B\rho$, a measure of the non-Darcy flow. For a high enough flow velocity, the discharge rate through a porous material no longer follows Darcy's law, and flow becomes nonlinear with the non-Darcy flow Equation given by

$$-\nabla P = \frac{\mu}{\kappa} v + B\rho v^2 \quad (4.2)$$

where v is the flow velocity, μ is the fluid viscosity, and κ is the permeability [6].

To measure flow resistance, the experimental setup consisted of a 20 ft PVC tube with an 8 in diameter (Figure 4.2). The tube has an empty chamber at both ends to allow for accurate

pressure measurement. The rest of the tube is filled with test material. Each measurement chamber is separated from the test material chamber by a wooden spacer with holes drilled through it to allow air to pass. The pressure is measured between ports approximately 4 in above the bottom of the tube and 4 in below the top of the tube using a pressure gauge with an appropriate range for each experiment. To create the pressure gradient, the bottom port is fed by an air compressor passing through one of several flow meters with ball float indicators. The complete experimental setup is shown in Figure 4.2.

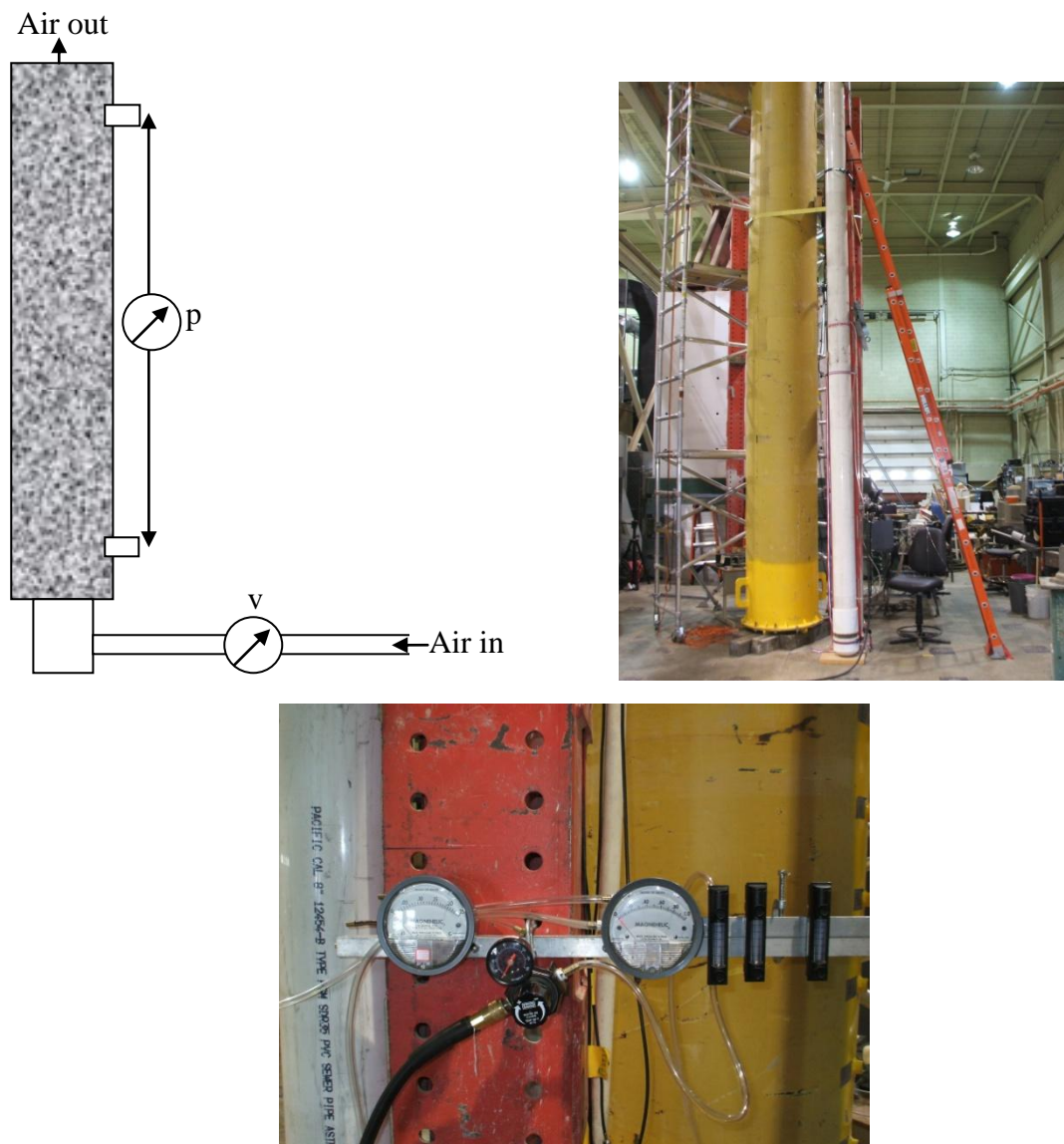


Figure 4.2: Flow resistivity test setup (left), PVC tube (right), and measurement apparatus (bottom).

4.3.1 Crushed Limestone

The flow resistivity data for crushed limestone is shown in Figure 4.3. The FL819 flow meter with a range of 2-30 L/min was used in this experiment. A Magnehelic pressure gauge with a range of 0-0.25 in of water was used to calculate the pressure gradient. The pressure drop was measured across the tube for the following flow rates: 2, 3, 4, 5, 6, 7, 8, 9, 10, 12, 14, 16, 18, 20, and 22 L/min. The resulting flow resistivity value is $300.5 \text{ N}\cdot\text{s}/\text{m}^4$ and the $\beta\rho$ value is 3717.3. The complete data used to generate Figure 4.3 is found in Appendix C.

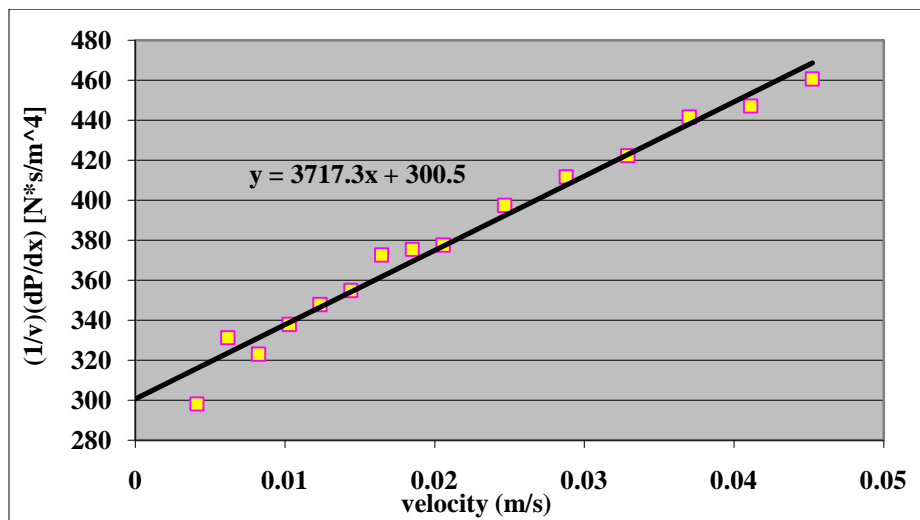


Figure 4.3: Crushed limestone flow resistivity result.

4.3.2 Non-Sifted Pea Gravel

The flow resistivity data for non-sifted pea gravel are plotted in Figure 4.4. Pressure measurements were taken with a Durablock Manometer with a range of 0-5 in of water. Flow rate measurements were taken using a FL819 flow meter with a range of 2-30 L/min. The resulting flow resistivity value is $1356.1 \text{ N}\cdot\text{s}/\text{m}^4$. The value for $\beta\rho$ is 12678. The complete data used to create Figure 4.4 may be found in Appendix C.

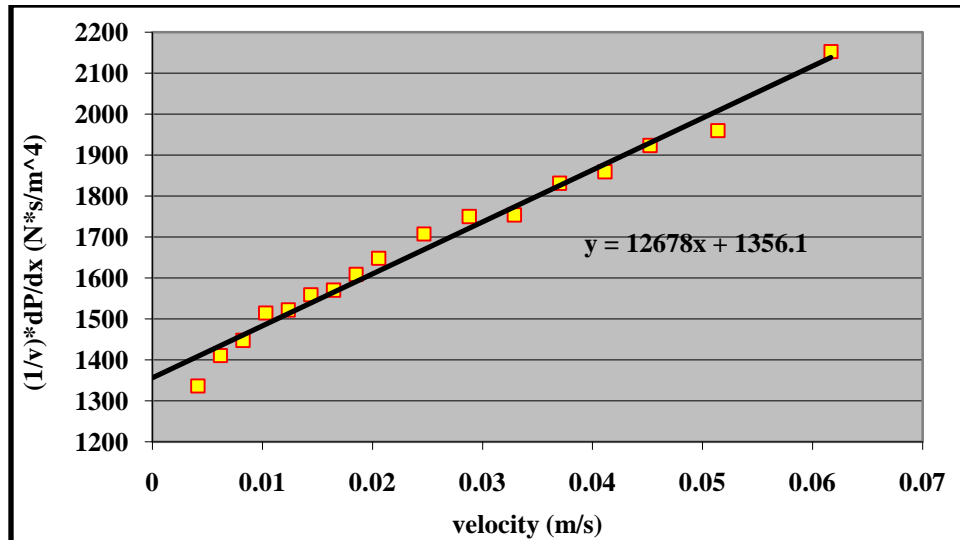


Figure 4.4: Non-sifted pea gravel flow resistivity result.

4.3.3 Sifted Large Pea Gravel

Figure 4.5 below shows the experimental flow resistivity results for a sample of large sifted pea gravel with depth 17 ft 4 in. In this experiment, air was fed into the 8 in PVC pipe through a perforated 3/4 in plywood base, covered by a 1/8 in wire mesh to prevent gravel particles from passing through. Pressure measurements were taken with a Magnahelic differential air pressure gauge with a range of 0-0.25 in of water. Flow rate measurements were taken with an Omega volumetric flow velocity sensor with variable area type ball float indicator. Three gauges and ranges were used. The resulting flow resistivity value is 429.93 N·s/m⁴. The value for $\beta\rho$ is 5961.8. The complete data used to create Figure 4.4 may be found in Appendix C.

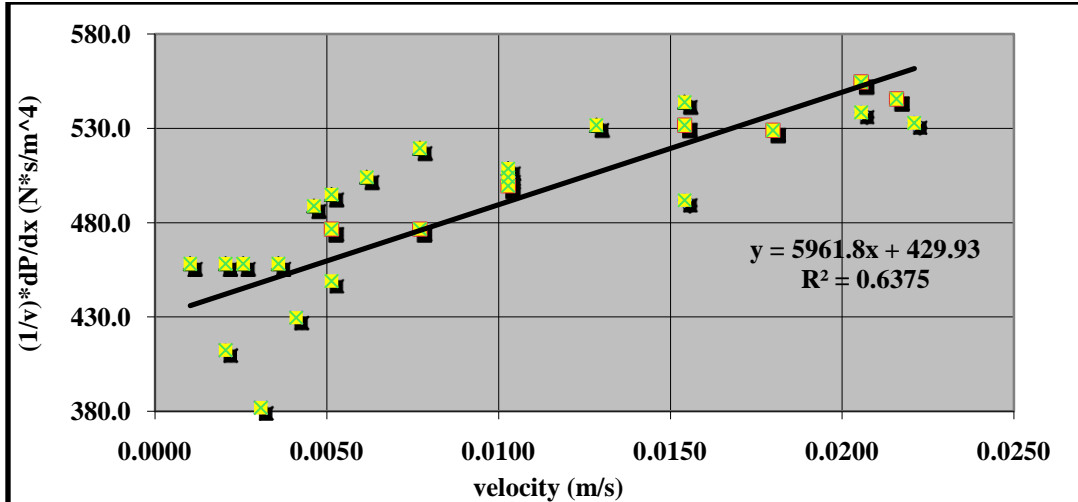


Figure 4.5: Screened large pea gravel, 17 ft 4 in depth.

4.3.4 10 mm Diameter Spheres

The flow resistivity data for the 10 mm glass spheres is plotted below in Figure 4.6. The pressure measurements were taken with a Durablock manometer with a range of 0-5 in of water. The flow rate measurements were taken with a FL820 flow meter with a range of 5-50 L/min. The static flow resistivity has a value of $219.35 \text{ N} \cdot \text{s/m}^4$ and the value for $\beta\mu$ is 3376.6. The data used to create Figure 4.6 is given in Appendix C.

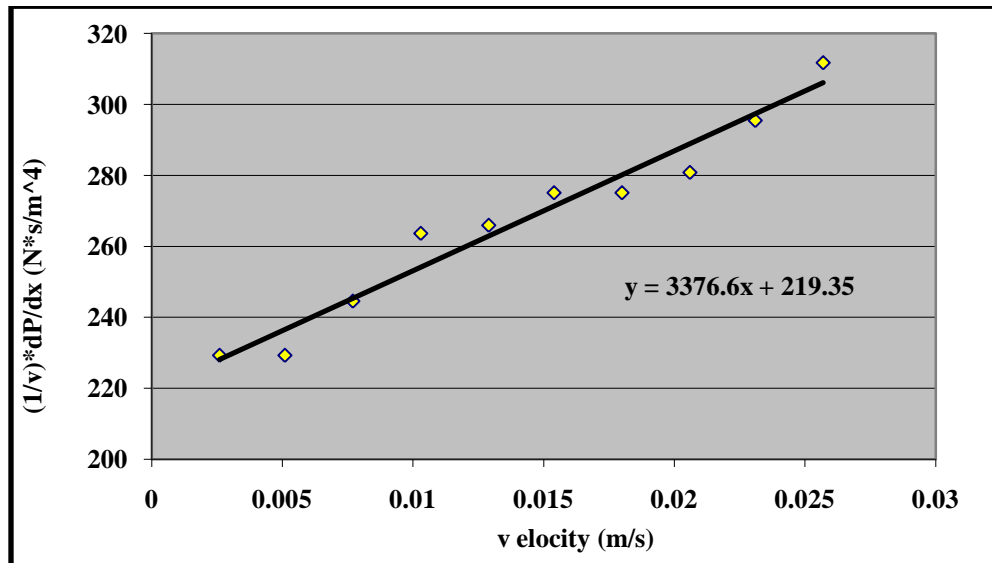


Figure 4.6: 10 mm glass spheres flow resistivity result.

CHAPTER 5

Results and Conclusions

Within the group of materials tested, it appears that there is a relationship between the attenuation coefficient of a material sample and its flow resistivity. The materials with higher experimental α values also had higher flow resistivity values, as shown in Table 5.1.

Table 5.1: Attenuation Coefficient and Flow Resistivity Comparison

Material	Attenuation Coefficient (200 Hz)	Flow Resistivity ($N \cdot s/m^4$)
Non-Sifted Pea Gravel	1.09	1356.1
Large Sifted Pea Gravel	0.80	429.93
Limestone	0.53	300.5
Glass Spheres	0.35	219.35

It is also interesting to note that the materials listed in Table 5.1 are arranged according to increasing particle uniformity. The non-sifted pea gravel with the highest attenuation has a large range of particle sizes and shapes, while the glass spheres with the lowest attenuation feature identical particles resulting in a well-defined lattice structure when sufficiently far away from the chamber walls.

Unfortunately, the available data do not suggest a clear relationship between the physical parameters and the measured wavelengths. This could perhaps be due to the observed wavelength, porosity, and tortuosity values for the different media being very similar.

Particularly in the case of the glass spheres, it was evident during experimentation that the pattern in which the particles stacked upon one another inside the test chambers influenced the results. For example, while using a transparent graduated cylinder to calculate porosity

values, significant void spaces were observed. For the purpose of our experiments, the test chambers were shaken to collapse these void spaces. However, since they appeared in the smaller test chambers used for calculating physical parameters, it is likely that similar void spaces also existed in the impedance tube where they could not be seen.

Another packing effect may be seen in Figure 5.1. It is clear that in a test chamber of any size, the particles are arranged uniformly in the center. As the particles come into proximity with the rigid chamber wall, they are no longer able to maintain their lattice structure and larger spaces are left between particles. In test chambers with smaller cross-sectional areas, the region close to the chamber wall will represent a larger fraction of the entire test chamber, and test results will contain larger errors.

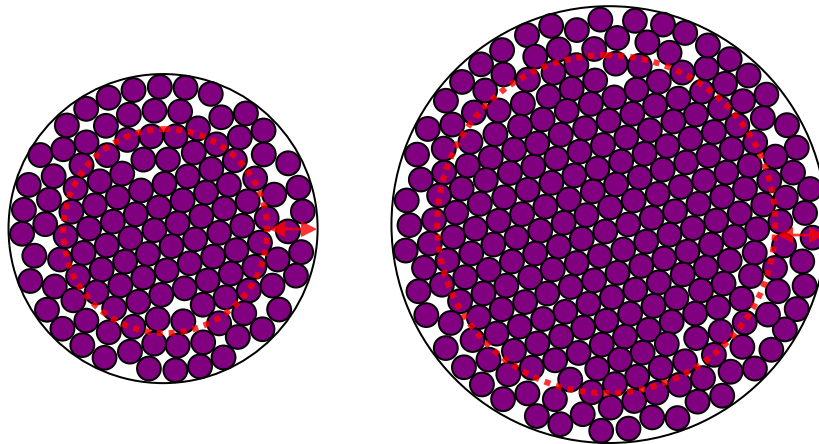


Figure 5.1: Sphere packing based on cell radius. Courtesy of Erica Lynn.

It is difficult to consider such packing effects in materials such as crushed limestone and pea gravel, which have particles with variable size and shape. It is possible that packing effects would not be a great concern in these materials because the smaller particles would fill in void spaces and the larger particles would have some ability to rotate and present a more appropriate shape to the lattice position.

Additionally, different material depths were tested for each material used. This was necessary due to the material quantities that were available. In particular, after the pea gravel was sifted into the large and small samples, there were only two meters of small pea gravel available for use in the impedance tube. Therefore, if the acoustic parameters vary significantly with material depth, the data sets cannot be adequately compared.

The work presented in this thesis could be expanded on by exploring other media with different properties to evaluate the consistency of the trends demonstrated so far. It may also be useful to study how the diameter of the test chamber affects the measured physical parameters described in Chapter 4. Particularly in the case of the glass spheres, an understanding of the lattice structure would be useful in analyzing the results.

A more elegant method for fitting the parameters of the wave Equation to the collected data would also be beneficial for continuing this work. The MMSE fitting method described in Chapter 3 was effective and produced good fits, but it is extremely inefficient and time consuming. The problem with this method is that it gets stuck on local minima. If the operator makes the search criteria too sparse, the program is likely to return a local minimum and, therefore, an inaccurate fit. If the operator makes the search criteria too dense, the program requires a very long time to run.

REFERENCES

- [1] T. Eggerding, "Parameters of acoustic propagation through porous media," M.S. thesis, University of Illinois at Urbana-Champaign, Urbana, Illinois, 2007.
- [2] T. Onder, "Low-frequency sound wave behavior in porous media," M.S. thesis, University of Illinois at Urbana-Champaign, Urbana, Illinois, 2008.
- [3] R. K. Moore, *Traveling-Wave Engineering*. New York, NY: McGraw-Hill, 1960, pp. 155-180.
- [4] A. D. Pierce, *Acoustics: An Introduction to its Physical Principles and Applications*. New York, NY: Acoustical Society of America, 1994, pp. 100-122.
- [5] R. Lee, "Absorption of low-frequency sound energy by vegetation: A laboratory investigation," M.S. thesis, University of Illinois at Urbana-Champaign, Urbana, Illinois, 2005.
- [6] X. Wang, F. Thauvin, and K. K. Mohanty, "Non-Darcy flow through anisotropic porous media," *Chemical Engineering Science*, vol. 54, no. 12, pp. 1859-1869, June 1999.

APPENDIX A

Impedance Tube Data

This appendix contains the discrete-frequency sound pressure amplitudes for experiments in the various materials.

A.1 Large Sifted Pea Gravel

Impedance Tube Data: 7 Oct 2008

1 m Depth Large Sifted Pea Gravel

Port	Height (m)	25 Hz	50 Hz	75 Hz	100 Hz	150 Hz	200 Hz
5	6.257	37.193	8.8932	39.8311	25.769	34.4149	6.4079
6	6.054	27.8705	11.5303	35.8039	15.6513	36.3867	5.0165
7	5.853	28.9151	19.7391	42.9527	9.6768	40.9135	13.93
8	5.651	22.0011	23.2343	36.2092	6.4804	24.4571	14.1511
9	5.448	17.0935	27.4464	30.0243	14.6259	9.8333	8.5325
10	5.248	13.4863	33.2961	24.0688	24.0949	23.1555	3.7938
11	5.047	9.1377	36.119	15.7805	29.8595	38.7627	11.9069
12	4.845	7.003	37.2353	11.5685	31.2981	43.5447	15.2486
13	4.645	9.8982	41.2956	18.2825	32.0008	40.5184	12.499
14	4.441	13.5894	37.3704	25.5873	23.6537	21.0965	3.5293
15	4.238	19.4737	37.0608	35.2091	15.706	11.9855	10.1787
16	4.038	23.3248	31.4085	38.5911	6.2723	27.4888	14.8325
17	3.84	28.8348	27.8373	42.645	10.1706	41.1972	13.3672
18	3.64	31.0305	20.9875	39.5869	18.0105	39.9684	5.1064
19	3.441	38.0581	17.1834	39.9517	26.6916	33.2191	6.9942
20	3.237	42.3325	11.7092	34.464	30.7275	15.831	14.1792
21	3.034	46.6408	7.8248	27.0765	30.983	14.957	14.6942
22	2.829	48.4571	7.7377	14.3715	25.2978	31.3243	7.6101
23	2.629	53.4176	13.4671	11.9863	19.9522	42.9402	4.4884
24	2.425	58.102	19.8023	14.3812	10.5937	41.8149	12.7219
25	2.223	58.5474	24.4724	22.0198	6.0154	28.9949	15.3326
26	2.023	60.3044	28.9194	30.0462	13.9477	11.596	10.3662
27	1.818	61.5032	33.1009	37.1618	22.9274	19.9352	3.1327
28	1.616	63.2604	36.0424	41.5012	28.954	36.4424	10.6048
29	1.414	62.7923	37.5862	42.9072	31.4233	44.1193	15.5337
30	1.212	58.3017	39.9934	32.6972	24.9866	36.727	12.9082
31	1.012	51.1441	41.8379	32.4105	17.6757	33.6768	9.1015
32	0.811	45.8073	42.9901	39.8039	16.7995	27.9755	8.972
33	0.611	34.7797	36.6897	40.61	18.8866	18.9056	6.8881
34	0.41	24.0365	28.0933	35.6557	19.3585	22.5585	5.7177
35	0.2	13.9231	17.788	24.6203	14.8749	21.3092	5.3862

Impedance Tube Data: 28 Oct 2008
 2 m Depth Large Sifted Pea Gravel

Port	Height (m)	25 Hz	50 Hz	75 Hz	100 Hz	150 Hz	200 Hz
5	6.257	6.2242	36.4381	20.5358	32.4105	27.0797	7.6419
6	6.054	7.6562	36.1491	14.1677	34.6222	34.5489	13.1523
7	5.853	10.0371	37.6592	13.8042	35.3378	35.2365	13.7596
8	5.651	12.0044	35.747	18.1381	29.7003	24.5397	7.5617
9	5.448	14.2181	33.4186	24.3812	21.4317	10.7005	5.2959
10	5.248	17.365	31.7266	31.3696	13.0351	16.3671	12.3848
11	5.047	20.1113	28.4878	36.702	11.2544	31.0882	14.9687
12	4.845	22.0164	23.2883	38.2189	19.6103	37.3463	10.0711
13	4.645	25.1218	18.942	39.2541	29.8589	35.2457	4.5006
14	4.441	26.6407	13.7117	35.1719	35.388	21.7706	10.9958
15	4.238	27.9867	10.8806	29.4666	36.7239	9.6117	14.7763
16	4.038	29.6474	11.8849	22.597	33.645	20.4807	11.743
17	3.84	31.2967	15.8976	16.3087	27.2839	32.8531	4.897
18	3.64	31.9042	20.4232	13.0159	17.6521	36.0042	8.332
19	3.441	34.3183	26.0449	16.7609	10.503	30.8838	14.1429
20	3.237	35.1292	30.5037	23.347	14.2164	17.0587	13.2813
21	3.034	36.2053	34.182	29.9052	23.8195	10.8958	6.5359
22	2.829	37.1466	36.9322	35.1213	32.1245	25.7428	7.014
23	2.629	37.4885	38.3358	38.0174	36.6476	36.7264	14.3887
24	2.425	37.0239	36.6858	36.2623	34.1709	36.1863	15.8555
25	2.223	37.535	33.1668	35.0925	27.1026	25.8177	10.7856
26	2.023	37.8031	31.4897	37.7936	26.415	24.0142	8.994
27	1.818	36.7475	29.5274	38.2281	27.0064	24.1258	9.215
28	1.616	34.2993	26.2323	32.5054	25.9744	21.3317	7.373
29	1.414	32.6933	27.5528	26.7659	25.3937	19.718	7.2264
30	1.212	28.5099	28.3958	18.9218	19.0435	15.2216	5.6358
31	1.012	24.8095	29.9283	18.8579	13.7531	13.9952	4.9661
32	0.811	21.4852	30.0466	22.4833	12.8487	11.7281	4.3655
33	0.611	16.4592	25.9968	23.3075	14.5024	8.2418	3.3937
34	0.41	11.5668	20.3134	21.0946	15.1573	9.415	2.8254
35	0.2	6.5749	12.5566	14.4957	11.4563	8.9246	2.1295

Impedance Tube Data: 4 Nov 2008
 4 m Depth Large Sifted Pea Gravel

Port	Height (m)	25 Hz	50 Hz	75 Hz	100 Hz	120 Hz	150 Hz	170 Hz	200 Hz
5	6.257	16.0955	15.0631	24.6661	16.6821	6.8979	25.055	16.3835	6.766
6	6.054	18.2283	11.0704	23.8441	24.1045	6.5441	20.6865	21.3758	7.6471
7	5.853	18.9316	7.1835	19.8628	27.0538	12.9178	10.3368	17.8527	14.0131
8	5.651	20.4345	6.5759	15.6656	27.661	18.2351	7.2141	9.6593	14.6555
9	5.448	20.9969	8.8851	10.2545	23.8346	19.5919	15.919	6.2097	8.4484
10	5.248	26.1597	14.7367	6.7073	21.2091	21.1877	25.7543	16.8573	5.7226
11	5.047	25.9663	18.2575	6.2156	12.0204	15.2526	24.9775	21.3782	13.0844
12	4.845	28.6861	23.5811	11.8115	6.4125	8.6893	19.7236	20.5138	17.166
13	4.645	29.223	26.793	17.2884	12.5386	5.9805	8.8574	11.5736	12.4686
14	4.441	28.8145	28.356	21.1697	20.5485	12.6553	10.1377	6.521	4.897
15	4.238	30.4074	31.2974	25.2441	27.982	19.6564	21.1194	16.44	11.5065
16	4.038	30.7947	32.0474	26.595	31.0848	22.8091	26.8099	22.4207	16.8634
17	3.84	27.0247	28.3137	23.3413	28.8113	21.5623	26.1511	22.9405	16.6551
18	3.64	21.8467	22.7925	18.0668	21.8602	16.9151	19.4844	17.0389	14.1535
19	3.441	20.0617	20.7424	16.1174	17.2156	13.8255	15.492	12.457	9.3062
20	3.237	20.1531	20.572	16.062	15.91	12.5116	14.9699	12.7648	9.0432
21	3.034	20.2247	19.7472	15.1209	15.1324	10.9621	12.6532	10.7895	8.6893
22	2.829	20.5439	18.6605	13.599	15.0271	10.5773	11.0967	8.5777	6.572
23	2.629	21.265	17.803	12.2021	14.6323	10.6353	11.4438	9.1506	6.2859
24	2.425	21.1072	15.6617	10.1258	11.8968	8.8522	9.8609	8.3485	6.3524
25	2.223	21.8525	14.1958	9.7634	9.5994	7.1106	7.4028	6.2093	4.4603
26	2.023	21.8609	13.0846	10.1587	9.0509	6.625	6.606	5.3709	3.7182
27	1.818	22.0135	12.3712	10.4114	9.2626	6.4568	6.5561	5.0326	4.0481
28	1.616	17.8586	9.3841	7.7281	7.5082	4.8795	4.8553	3.823	2.4869
29	1.414	19.6105	10.9744	7.283	8.2099	5.5075	4.8415	4.1789	2.3364
30	1.212	18.1245	11.7709	5.4262	6.4954	4.564	3.832	2.7497	2.3606
31	1.012	16.6739	12.8673	5.1976	4.9424	3.5729	3.9471	2.9111	1.9224
32	0.811	15.9094	14.018	6.3687	4.7704	3.2958	3.5996	3.1716	1.5546
33	0.611	11.0868	10.8963	5.913	4.6939	3.0709	2.0274	1.5256	1.2983
34	0.41	7.6783	8.29	5.3627	4.8684	2.9654	2.4895	1.8683	1.0526
35	0.2	4.5554	5.284	4.048	3.9694	2.1114	2.6126	2.0233	1.1307

A.2 10 mm Glass Spheres

Impedance Tube Data: 4 Nov 2009

1 m Depth 10 mm Glass Spheres

Port	Height (m)	25 Hz	50 Hz	75 Hz	100 Hz	120 Hz	150 Hz	170 Hz	200 Hz
6	6.054	96.8006	21.6115	8.9783	4.5573	0.5138	0.982	3.1388	2.31
7	5.853	86.9327	15.2413	8.5297	3.4867	1.8468	3.1275	2.9745	1.941
8	5.651	87.6855	13.0504	8.7506	2.3774	3.7302	4.9184	2.0297	1.7787
9	5.448	74.5858	13.4808	7.2702	0.8753	4.458	4.6716	0.5991	1.9532
10	5.248	68.1334	19.0046	6.3245	1.6184	4.7368	3.4842	2.1007	2.3825
11	5.047	58.4463	25.19	5.2585	3.1266	3.9502	1.1889	3.2298	2.213
12	4.845	50.3039	32.7549	5.0507	4.5148	2.5304	1.8176	3.3419	1.862
13	4.645	38.3728	37.3845	5.4195	5.0359	0.6462	3.9483	2.056	1.9183
14	4.441	24.7753	38.5268	6.0087	4.6336	1.6385	4.6208	0.5653	2.1623
15	4.238	17.1564	44.7413	7.6185	4.286	3.4427	4.5371	2.0422	2.291
16	4.038	9.4071	47.0065	8.5961	3.1162	4.5046	2.882	3.1871	1.8754
17	3.84	11.1116	46.7857	9.0847	1.5649	4.7146	0.5911	3.1942	1.7668
18	3.64	20.6808	46.1325	9.23	0.9216	4.0694	2.453	2.0476	2.2139
19	3.441	30.4379	42.7897	8.6045	2.3074	2.5811	4.2378	0.5925	2.3131
20	3.237	41.4374	39.7094	7.9198	3.7988	0.8002	5.0161	2.0281	2.0155
21	3.034	49.4166	33.5997	6.5372	4.6077	1.483	4.0534	3.1119	1.6833
22	2.829	62.2229	28.8412	5.5671	5.0813	3.3104	2.12	3.2189	2.107
23	2.629	69.5396	22.1449	4.8145	4.6909	4.38	0.747	2.0773	2.3612
24	2.425	78.056	16.1699	5.0069	3.7613	4.7198	3.0839	0.6004	2.1257
25	2.223	86.4153	12.5481	6.0107	2.404	4.2036	4.6965	1.9803	1.7596
26	2.023	92.9107	14.2417	7.5624	0.9606	2.9606	5.1363	3.3421	2.059
27	1.818	100.5684	18.4709	8.1997	1.5535	0.9395	3.5986	3.1971	2.3253
28	1.616	107.2581	24.9276	9.0031	3.0928	1.3215	1.4025	2.1078	2.2452
29	1.414	109.8734	30.4627	9.0296	4.212	3.0448	1.4627	0.5877	1.7609
30	1.212	114.4225	36.2092	8.8445	4.9117	4.3037	3.6771	1.9333	1.8134
31	1.012	116.2244	40.5042	8.0644	4.9012	4.7027	4.8443	3.1318	2.2539
32	0.811	125.4157	54.3885	5.6714	2.7793	3.5319	4.9005	4.4254	4.6967
33	0.611	130.5857	68.6412	10.9754	1.3484	1.2414	2.9709	3.4275	5.6493
34	0.41	135.678	81.086	17.3069	3.6603	2.0095	0.9831	0.7487	2.2649

Impedance Tube Data: 7 Dec 2009

1.8 m Depth 10 mm Glass Spheres

Port	Height (m)	25 H	50 Hz	75 Hz	100 Hz	120 Hz	150 Hz	170 Hz	200 Hz
8	5.853	0.4379	0.6231	0.3301	0.1321	0.2058	0.0413	0.1112	0.0691
9	5.651	0.4128	0.6701	0.2538	0.2044	0.138	0.0951	0.1145	0.067
10	5.448	0.3891	0.7123	0.1575	0.2982	0.1263	0.1928	0.0797	0.1392
11	5.248	0.3094	0.6316	0.0564	0.3243	0.1823	0.2122	0.0347	0.1405
12	5.047	0.2745	0.6179	0.1226	0.3557	0.2636	0.1955	0.08	0.0961
13	4.845	0.225	0.551	0.2317	0.3285	0.2974	0.1121	0.1179	0.0523
14	4.645	0.199	0.5109	0.354	0.2906	0.3077	0.0377	0.1256	0.1252
15	4.441	0.1577	0.386	0.4038	0.1904	0.2294	0.1267	0.076	0.1496
16	4.238	0.1014	0.1988	0.3055	0.091	0.1016	0.1378	0.0245	0.079
17	4.038	0.1707	0.2104	0.4564	0.1617	0.1139	0.2176	0.0788	0.0509
18	3.84	0.2092	0.1766	0.4381	0.241	0.1778	0.1745	0.1178	0.096
19	3.64	0.2552	0.2165	0.384	0.3127	0.2563	0.0817	0.1173	0.1476
20	3.441	0.3031	0.2982	0.2995	0.349	0.2964	0.0562	0.076	0.1319
21	3.237	0.3454	0.3824	0.1903	0.3384	0.2833	0.1508	0.0349	0.064
22	3.034	0.3844	0.4707	0.0859	0.303	0.2362	0.2125	0.0795	0.0748
23	2.829	0.4451	0.5594	0.0824	0.2353	0.1594	0.2132	0.1196	0.1392
24	2.629	0.4874	0.6165	0.1878	0.1577	0.1132	0.1497	0.1167	0.1432
25	2.425	0.518	0.6496	0.2893	0.1342	0.1676	0.0506	0.0753	0.0864
26	2.223	0.5665	0.6836	0.3788	0.1979	0.2472	0.0876	0.0359	0.0575
27	2.023	0.6431	0.7356	0.4689	0.2974	0.3165	0.1924	0.0864	0.1336
28	1.818	0.6584	0.6923	0.4814	0.348	0.306	0.2298	0.1235	0.1545
29	1.616	0.7567	0.4977	0.4662	0.4875	0.2129	0.1972	0.1643	0.1176
30	1.414	0.8178	0.2998	0.3764	0.5573	0.3131	0.1	0.1322	0.1763
31	1.212	0.8506	0.2496	0.25	0.5065	0.3928	0.0979	0.0568	0.1391
32	1.012	0.9933	0.4078	0.1413	0.4186	0.4176	0.1795	0.0972	0.0608
33	0.811	1.0227	0.5686	0.1004	0.206	0.2815	0.179	0.1387	0.1372
34	0.41	1.1186	0.8573	0.328	0.3229	0.186	0.0388	0.0187	0.0493
35	0.2	1.0792	0.8928	0.3888	0.4697	0.3478	0.1422	0.0981	0.102
36	0	1.1741	0.9909	0.4463	0.5664	0.4412	0.1992	0.1499	0.1799

Impedance Tube Data: 4 Jan 2010

3 m Depth 10 mm Glass Spheres

Port	Height (m)	25 Hz	50 Hz	75 Hz	100 Hz	120 Hz	150 Hz	170 Hz	200 Hz
7	5.853	0.1752	0.7796	0.6145	0.1978	0.668	0.0956	0.1731	0.1286
8	5.651	0.1944	0.7306	0.7368	0.1325	0.6225	0.1013	0.1098	0.2271
9	5.448	0.2203	0.6735	0.837	0.0876	0.4844	0.1891	0.063	0.2614
10	5.248	0.2214	0.5248	0.791	0.1175	0.2595	0.2234	0.1293	0.1703
11	5.047	0.2455	0.4205	0.7741	0.1928	0.2506	0.2213	0.189	0.1151
12	4.845	0.2571	0.2846	0.6668	0.2478	0.4432	0.1535	0.1782	0.2049
13	4.645	0.2698	0.1702	0.5305	0.2764	0.6124	0.0825	0.1117	0.2552
14	4.441	0.2853	0.1524	0.3816	0.2756	0.6954	0.128	0.0608	0.2049
15	4.238	0.2847	0.2506	0.2624	0.2352	0.6427	0.2035	0.1333	0.1139
16	4.038	0.3219	0.4084	0.3104	0.1827	0.5193	0.249	0.1998	0.1902
17	3.84	0.3122	0.5155	0.4338	0.1035	0.2881	0.206	0.1809	0.2551
18	3.64	0.311	0.623	0.5827	0.09	0.2351	0.1278	0.1124	0.2275
19	3.441	0.3159	0.7243	0.7157	0.1546	0.4265	0.0829	0.0607	0.133
20	3.237	0.3115	0.7844	0.7865	0.2186	0.597	0.1501	0.1297	0.1454
21	3.034	0.3136	0.8569	0.8451	0.2696	0.7012	0.2197	0.1872	0.2331
22	2.829	0.2778	0.8805	0.7066	0.3054	0.5779	0.2663	0.1709	0.2937
23	2.629	0.2429	0.9021	0.5927	0.3291	0.5262	0.2798	0.1649	0.3467
24	2.425	0.2167	0.8748	0.5951	0.3063	0.6424	0.2162	0.1822	0.2506
25	2.223	0.2262	0.8569	0.7647	0.2586	0.7893	0.1646	0.182	0.2215
26	2.023	0.238	0.7107	0.8749	0.169	0.6954	0.197	0.1218	0.2793
27	1.818	0.3229	0.6487	1.0964	0.1826	0.539	0.2771	0.1412	0.2481
28	1.616	0.3077	0.3662	0.867	0.215	0.2714	0.1924	0.1547	0.1267
29	1.414	0.3483	0.2294	0.7366	0.2616	0.4148	0.102	0.1296	0.2021
30	1.212	0.3846	0.2002	0.5214	0.2554	0.5621	0.1051	0.0584	0.1754
31	1.012	0.4144	0.303	0.2726	0.1963	0.5549	0.1796	0.096	0.0697
32	0.811	0.4474	0.4462	0.1992	0.1028	0.3955	0.1888	0.1432	0.1677
34	0.41	0.5163	0.7132	0.6977	0.1654	0.2737	0.0431	0.0203	0.0667
35	0.2	0.4687	0.699	0.7786	0.2272	0.483	0.1489	0.1006	0.1234
36	0	0.5179	0.7874	0.9073	0.2784	0.6224	0.212	0.1559	0.2227

Impedance Tube Data: 11 Jan 2010

3.8 m Depth 10 mm Glass Spheres

Port	Height (m)	25 Hz	50 Hz	75 Hz	100 Hz	120 Hz	150 Hz	170 Hz	200 Hz
7	5.853	0.1655	0.5124	0.3923	0.7957	0.0661	0.3831	0.1319	0.0774
8	5.651	0.1849	0.4494	0.3663	0.9812	0.1144	0.2525	0.1337	0.1891
9	5.448	0.2208	0.4638	0.3402	1.1363	0.1837	0.1318	0.0951	0.2523
10	5.248	0.2106	0.4407	0.2275	0.9325	0.1915	0.2413	0.0362	0.1586
11	5.047	0.2225	0.5123	0.145	0.7338	0.1869	0.3836	0.0898	0.0648
12	4.845	0.2308	0.6019	0.0966	0.4493	0.1495	0.4243	0.134	0.1614
13	4.645	0.2402	0.7031	0.1449	0.225	0.0962	0.3545	0.1327	0.2279
14	4.441	0.2429	0.7828	0.2264	0.3887	0.0659	0.1965	0.084	0.1873
15	4.238	0.2426	0.856	0.3051	0.6797	0.1078	0.1369	0.0362	0.0767
16	4.038	0.2525	0.9161	0.3647	0.9018	0.1603	0.295	0.0912	0.1294
17	3.84	0.2529	0.9436	0.3969	1.0084	0.189	0.4042	0.1324	0.2111
18	3.64	0.2321	0.9003	0.4036	0.9296	0.1872	0.4352	0.1275	0.1969
19	3.441	0.2104	0.9496	0.4032	0.7679	0.1989	0.4157	0.1117	0.2051
20	3.237	0.1816	1.0303	0.3661	0.613	0.1967	0.3247	0.1074	0.2031
21	3.034	0.1441	1.0927	0.2913	0.5673	0.1583	0.2472	0.0951	0.1378
22	2.829	0.1355	1.2434	0.2572	0.708	0.133	0.311	0.0876	0.1424
23	2.629	0.0968	1.1189	0.1758	0.6254	0.0963	0.2708	0.0624	0.1334
24	2.425	0.1029	1.2409	0.2109	0.7163	0.1422	0.2583	0.0844	0.1152
25	2.223	0.1076	1.2215	0.2722	0.6085	0.1761	0.1964	0.0888	0.1038
26	2.023	0.1109	0.9971	0.3062	0.3926	0.153	0.2297	0.0598	0.1376
27	1.818	0.1326	0.8026	0.3384	0.3746	0.1052	0.2896	0.0581	0.112
28	1.616	0.1533	0.5494	0.3245	0.5315	0.0637	0.2465	0.0789	0.0704
29	1.414	0.1637	0.3245	0.2597	0.6088	0.0918	0.1244	0.0644	0.1021
30	1.212	0.1843	0.2874	0.1875	0.605	0.1267	0.1252	0.0301	0.0907
31	1.012	0.1996	0.436	0.0987	0.4665	0.1263	0.2183	0.0457	0.0347
32	0.811	0.2115	0.629	0.0706	0.2384	0.0881	0.2265	0.0688	0.0823
33	0.611	0.2167	0.7873	0.1468	0.1275	0.0278	0.1275	0.0516	0.0926
34	0.41	0.2293	0.9448	0.2314	0.3626	0.0567	0.0473	0.0092	0.0314
35	0.2	0.2308	1.0262	0.2861	0.5526	0.1115	0.1848	0.0503	0.0647
36	0	0.2463	1.1167	0.3219	0.6534	0.1389	0.2545	0.0757	0.1128

APPENDIX B

Experimental Tortuosity Data

B.1 Non-Sifted Pea Gravel Tortuosity Results

Test 1: Non-Sifted Pea Gravel + Salt Water (35 g salt / L H ₂ O)				
R _l (Ω)	V _t (v)	V _r (v)	R _t =R _r *V _t /V _r (Ω)	Height(m)
18.7	5.865	1.585	69.20	0.705
Test 1: Salt Water (35g salt /L H ₂ O)				
R _l (Ω)	V _t (v)	V _r (v)	R _t =R _r *V _t /V _r (Ω)	Height(m)
18.7	1.746	6.280	5.199	0.228
Porosity = 0.35				
Tortuosity = porosity*R(gravel & H ₂ O)/R(H ₂ O) = 1.485				

Test 2: Non-Sifted Pea Gravel + Salt Water (35 g salt / L H ₂ O)				
R _l (Ω)	V _t (v)	V _r (v)	R _t =R _r *V _t /V _r (Ω)	Height(m)
18.7	3.747	1.013	69.17	0.705
Test 2: Salt Water (35g salt /L H ₂ O)				
R _l (Ω)	V _t (v)	V _r (v)	R _t =R _r *V _t /V _r (Ω)	Height(m)
18.7	1.161	4.130	5.257	0.228
Porosity = 0.35				
Tortuosity = porosity*R(gravel & H ₂ O)/R(H ₂ O) = 1.489				

Test 3: Non-Sifted Pea Gravel + Salt Water (35 g salt / L H ₂ O)				
R _l (Ω)	V _t (v)	V _r (v)	R _t =R _r *V _t /V _r (Ω)	Height(m)
18.7	2.021	0.547	69.09	0.705
Test 3: Salt Water (35g salt /L H ₂ O)				
R _l (Ω)	V _t (v)	V _r (v)	R _t =R _r *V _t /V _r (Ω)	Height(m)
18.7	0.680	2.415	5.265	0.228
Porosity = 0.35				
Tortuosity = porosity*R(gravel & H ₂ O)/R(H ₂ O) = 1.507				

Test 4: Non-Sifted Pea Gravel + Salt Water (35 g salt / L H ₂ O)				
R1(Ω)	Vt (v)	Vr (v)	Rt=Rr*Vt/Vr (Ω)	Height(m)
18.7	2.120	0.491	80.74	0.735
Test 4: Salt Water (35g salt /L H ₂ O)				
R1(Ω)	Vt (v)	Vr (v)	Rt=Rr*Vt/Vr (Ω)	Height(m)
18.7	0.708	2.144	6.175	0.250
Porosity = 0.35				
Tortuosity = porosity*R(gravel & H ₂ O)/R(H ₂ O) = 1.543				

Test 5: Non-Sifted Pea Gravel + Salt Water (35 g salt / L H ₂ O)				
R1(Ω)	Vt (v)	Vr (v)	Rt=Rr*Vt/Vr (Ω)	Height(m)
18.7	3.837	0.888	80.80	0.735
Test 5: Salt Water (35g salt /L H ₂ O)				
R1(Ω)	Vt (v)	Vr (v)	Rt=Rr*Vt/Vr (Ω)	Height(m)
18.7	1.168	3.545	6.161	0.250
Porosity = 0.35				
Tortuosity = porosity*R(gravel & H ₂ O)/R(H ₂ O) = 1.548				

B.2 Large Sifted Pea Gravel Tortuosity Results

Test 1: Large Sifted Pea Gravel + Salt Water (35 g salt / L H ₂ O)				
R1(Ω)	Vt (v)	Vr (v)	Rt=Rr*Vt/Vr (Ω)	Height(m)
19.8	5.28 v	0.25v	418.2	0.61
Test 1: Salt Water (35g salt /L H ₂ O)				
R1(Ω)	Vt (v)	Vr (v)	Rt=Rr*Vt/Vr (Ω)	Height(m)
19.8	4.53v	0.9v	99.7	0.61
Porosity = 0.42				
Tortuosity = porosity*R(gravel & H ₂ O)/R(H ₂ O) = 1.76				

Test 2: Large Sifted Pea Gravel + Salt Water (35 g salt / L H ₂ O)				
R1(Ω)	Vt (v)	Vr (v)	Rt=Rr*Vt/Vr (Ω)	Height(m)
19.8	5.26 v	0.267v	390.1	0.61
Test 2: Salt Water (35g salt /L H ₂ O)				
R1(Ω)	Vt (v)	Vr (v)	Rt=Rr*Vt/Vr (Ω)	Height(m)
19.8	4.53v	0.9v	99.7	0.61
Porosity = 0.42				
Tortuosity = porosity*R(gravel & H ₂ O)/R(H ₂ O) = 1.64				

Test 3: Large Sifted Pea Gravel + Salt Water (35 g salt / L H ₂ O)				
R1(Ω)	Vt (v)	Vr (v)	Rt=Rr*Vt/Vr (Ω)	Height(m)
19.8	5.27 v	0.256v	407.6	0.61
Test 3: Salt Water (35g salt /L H ₂ O)				
R1(Ω)	Vt (v)	Vr (v)	Rt=Rr*Vt/Vr (Ω)	Height(m)
19.8	4.53v	0.9v	99.7	0.61
Porosity = 0.42				
Tortuosity = porosity*R(gravel & H ₂ O)/R(H ₂ O) = 1.72				

Test 4: Large Sifted Pea Gravel + Salt Water (35 g salt / L H ₂ O)				
R1(Ω)	Vt (v)	Vr (v)	Rt=Rr*Vt/Vr (Ω)	Height(m)
19.8	5.27 v	0.234v	446	0.61
Test 4: Salt Water (35g salt /L H ₂ O)				
R1(Ω)	Vt (v)	Vr (v)	Rt=Rr*Vt/Vr (Ω)	Height(m)
19.8	4.53v	0.9v	99.7	0.61
Porosity = 0.42				
Tortuosity = porosity*R(gravel & H ₂ O)/R(H ₂ O) = 1.88				

Test 5: Large Sifted Pea Gravel + Salt Water (35 g salt / L H ₂ O)				
R1(Ω)	Vt (v)	Vr (v)	Rt=Rr*Vt/Vr (Ω)	Height(m)
19.8	5.24 v	0.263v	394.5	0.61
Test 5: Salt Water (35g salt /L H ₂ O)				
R1(Ω)	Vt (v)	Vr (v)	Rt=Rr*Vt/Vr (Ω)	Height(m)
19.8	4.53v	0.9v	99.7	0.61
Porosity = 0.42				
Tortuosity = porosity*R(gravel & H ₂ O)/R(H ₂ O) = 1.66				

B.3 10 mm Glass Spheres Tortuosity Results

Test 1: 10 mm Spheres + Salt Water (35 g salt / L H ₂ O)				
R1(Ω)	Vt (v)	Vr (v)	Rt=Rr*Vt/Vr (Ω)	Height(m)
19.8	5	3.33	28.08	0.635
Test 1: Salt Water (35g salt /L H ₂ O)				
R1(Ω)	Vt (v)	Vr (v)	Rt=Rr*Vt/Vr (Ω)	Height(m)
19.8	5	10.3	9.08	0.635
Porosity = 0.369				
Tortuosity = porosity*R(spheres & H ₂ O)/R(H ₂ O) = 1.14				

Test 2: 10 mm Spheres + Salt Water (35 g salt / L H ₂ O)				
R1(Ω)	Vt (v)	Vr (v)	Rt=Rr*Vt/Vr (Ω)	Height(m)
19.8	5.08	1.28	78.6	0.66
Test 2: Salt Water (35g salt /L H ₂ O)				
R1(Ω)	Vt (v)	Vr (v)	Rt=Rr*Vt/Vr (Ω)	Height(m)
19.8	5.06	4.60	21.78	0.66
Porosity = 0.369				
Tortuosity = porosity*R(spheres & H ₂ O)/R(H ₂ O) = 1.33				

Test 3: 10 mm Spheres + Salt Water (35 g salt / L H ₂ O)				
R1(Ω)	Vt (v)	Vr (v)	Rt=Rr*Vt/Vr (Ω)	Height(m)
19.8	5.07	1.45	69.2	0.66
Test 3: Salt Water (35g salt /L H ₂ O)				
R1(Ω)	Vt (v)	Vr (v)	Rt=Rr*Vt/Vr (Ω)	Height(m)
19.8	5.02	4.47	22.3	0.66
Porosity = 0.369				
Tortuosity = porosity*R(spheres & H ₂ O)/R(H ₂ O) = 1.145				

Test 4: 10 mm Spheres + Salt Water (35 g salt / L H ₂ O)				
R1(Ω)	Vt (v)	Vr (v)	Rt=Rr*Vt/Vr (Ω)	Height(m)
19.8	6.47	0.838	152.87	0.66
Test 4: Salt Water (35g salt /L H ₂ O)				
R1(Ω)	Vt (v)	Vr (v)	Rt=Rr*Vt/Vr (Ω)	Height(m)
19.8	5.14	2.13	47.78	0.66
Porosity = 0.369				
Tortuosity = porosity*R(spheres & H ₂ O)/R(H ₂ O) = 1.18				

Test 5: 10 mm Spheres + Salt Water (35 g salt / L H ₂ O)				
R1(Ω)	Vt (v)	Vr (v)	Rt=Rr*Vt/Vr (Ω)	Height(m)
19.8	6.45	0.839	152.22	0.66
Test 5: Salt Water (35g salt /L H ₂ O)				
R1(Ω)	Vt (v)	Vr (v)	Rt=Rr*Vt/Vr (Ω)	Height(m)
19.8	5.14	2.16	47.12	0.66
Porosity = 0.369				
Tortuosity = porosity*R(spheres & H ₂ O)/R(H ₂ O) = 1.19				

APPENDIX C

Experimental Flow Resistivity Data

C.1 Flow Resistivity Data for Crushed Limestone

Volume Velocity (L/m)	Pressure (inches H ₂ O)	Volume Velocity (m ³ /s)	Pressure (Pascal)	Port Separation (m)	Tube Cross Section (m ²)	Flow Velocity (m/s)	Gradient (Pascal/m)	Gradient/Flow Velocity
2	0.015	0.000033	3.74	5.28	0.0324	0.0041	1.23	298.12
3	0.025	0.000050	6.23			0.0062	2.04	331.24
4	0.033	0.000067	8.09			0.0082	2.66	322.96
5	0.043	0.000083	10.59			0.0103	3.47	337.87
6	0.053	0.000100	13.08			0.0123	4.29	347.81
7	0.063	0.000117	15.57			0.0144	5.11	354.90
8	0.075	0.000133	18.68			0.0164	6.13	372.65
9	0.085	0.000150	21.17			0.0185	6.95	375.41
10	0.095	0.000167	23.66			0.0206	7.76	377.62
12	0.120	0.000200	29.89			0.0247	9.81	397.49
14	0.145	0.000233	36.11			0.0288	11.85	411.69
16	0.170	0.000267	42.34			0.0329	13.89	422.33
18	0.200	0.000300	49.81			0.0370	16.34	441.66
20	0.225	0.000333	56.04			0.0411	18.39	447.18
22	0.255	0.000367	63.51			0.0452	20.84	460.73

C.2 Flow Resistivity Data for Non-Sifted Pea Gravel

Volume Velocity (L/m)	Pressure (inches H ₂ O)	Volume Velocity (m ³ /s)	Pressure (Pascal)	Port Separation (m)	Tube Cross Section (m ²)	Flow Velocity (m/s)	Gradient (Pascal/m)	Gradient/Flow Velocity
2	0.060	0.000033	14.93	5.28	0.0324	0.0041	5.49	1336.17
3	0.095	0.000050	23.64			0.0062	8.70	1410.40
4	0.130	0.000067	32.35			0.0082	11.90	1447.52
5	0.170	0.000083	42.30			0.0103	15.57	1514.32
6	0.205	0.000100	51.01			0.0123	18.77	1521.75
7	0.245	0.000117	60.97			0.0144	22.43	1558.86
8	0.282	0.000133	70.17			0.0164	25.82	1570.00
9	0.325	0.000150	80.87			0.0185	29.76	1608.35
10	0.370	0.000167	92.07			0.0206	33.88	1647.94
12	0.460	0.000200	114.47			0.0247	42.12	1707.33
14	0.550	0.000233	136.86			0.0288	50.36	1749.74
16	0.630	0.000267	156.77			0.0329	57.68	1753.72
18	0.740	0.000300	184.15			0.0370	67.76	1831.05
20	0.835	0.000333	207.79			0.0411	76.45	1859.50
22	0.950	0.000367	236.40			0.0452	86.98	1923.27
25	1.100	0.000417	273.73			0.0514	100.72	1959.71
30	1.450	0.000500	360.83			0.0617	132.76	2152.72

C.3 Flow Resistivity Data for Large Sifted Pea Gravel

Volume Velocity (L/m)	Pressure (inches H ₂ O)	Volume Velocity (m ³ /s)	Pressure (Pascal)	Port Separation (m)	Tube Cross Section (m ²)	Flow Velocity (m/s)	Gradient (Pascal/m)	Gradient/Flow Velocity
20	0.11	0.00033	27.4	5.28	0.0324	0.0103	5.2	504.1
30	0.161	0.00050	40.1			0.0154	7.6	491.9
40	0.235	0.00067	58.5			0.0206	11.1	538.5
43	0.25	0.00072	62.2			0.0221	11.8	532.9
10	0.052	0.00017	12.9			0.0051	2.4	476.6
15	0.078	0.00025	19.4			0.0077	3.7	476.6
20	0.109	0.00033	27.1			0.0103	5.1	499.5
30	0.174	0.00050	43.3			0.0154	8.2	531.6
35	0.202	0.00058	50.3			0.0180	9.5	529.0
40	0.242	0.00067	60.2			0.0206	11.4	554.5
42	0.25	0.00070	62.2			0.0216	11.8	545.6
2	0.01	0.00003	2.5			0.0010	0.5	458.3
4	0.02	0.00007	5.0			0.0021	0.9	458.3
5	0.025	0.00008	6.2			0.0026	1.2	458.3
7	0.035	0.00012	8.7			0.0036	1.6	458.3
9	0.048	0.00015	11.9			0.0046	2.3	488.8
10	0.054	0.00017	13.4			0.0051	2.5	494.9
12	0.066	0.00020	16.4			0.0062	3.1	504.1
15	0.085	0.00025	21.2			0.0077	4.0	519.4
20	0.111	0.00033	27.6			0.0103	5.2	508.7
25	0.145	0.00042	36.1			0.0129	6.8	531.6
30	0.178	0.00050	44.3			0.0154	8.4	543.8
2	0.0075	0.00003	1.9			0.0010	0.4	343.7
4	0.018	0.00007	4.5			0.0021	0.8	412.4
6	0.025	0.00010	6.2			0.0031	1.2	381.9
8	0.0375	0.00013	9.3			0.0041	1.8	429.6
10	0.049	0.00017	12.2			0.0051	2.3	449.1

C.4 Flow Resistivity Data for 10 mm Glass Spheres

Volume Velocity (L/m)	Pressure (inches H ₂ O)	Volume Velocity (m ³ /s)	Pressure (Pascal)	Port Separation (m)	Tube Cross Section (m ²)	Flow Velocity (m/s)	Gradient (Pascal/m)	Gradient/Flow Velocity
5	0.0125	0.0000833	3.1133	5.28	0.0324	0.0026	0.5896	229.2539
10	0.0275	0.0001667	6.8493			0.0051	1.2972	229.2539
15	0.04	0.00025	9.9626			0.0077	1.8869	244.5375
20	0.0575	0.0003333	14.3213			0.0103	2.7124	263.642
25	0.0725	0.0004167	18.0573			0.0129	3.4199	265.9346
30	0.09	0.0005	22.4159			0.0154	4.2454	275.1047
35	0.105	0.0005833	26.1519			0.018	4.953	275.1047
40	0.1225	0.0006667	30.5106			0.0206	5.7785	280.8361
45	0.145	0.00075	36.1146			0.0231	6.8399	295.4828
50	0.17	0.0008333	42.3412			0.0257	8.0192	311.7854

APPENDIX D

MATLAB Source Code

This Appendix contains the code needed to generate acoustic parameters from the raw data found in Appendix A. It is intended for use with MATLAB version R2007b.

D.1 byt_swr.m

```
function byt_swr(directory, depth, freqs,graphtitle)
%*****
%BYT_SWR
%Program for analyzing standing waves in the
%'Big Yellow Tube' at CERL.
%Written by Tim Eggerding 2006-2007
%Adapted from code written by Ryan Lee for the acoustic chamber
%updated for new datastructures by Todd Borrowman June 2009
%Inputs:
%  directory: Directory location where the compPres data is located
%  depth: Depth of the material sample, in meters
%  freqs: Array of frequencies to iterate over
%  graphtitle: Title of graph
%Outputs:
%  No return value
%  Displays graph of measured pressures, best-fit curve
%  Saves measured pressures, calculated parameters to file
%*****

%Constants for speed in the air, detailed location in the tube
l_tube = 7.25;
tube_axis = depth:0.01:l_tube;
c_air = 343;

cd(directory);
figure;
for i=1:length(freqs)
    freq = freqs(i);
    if(isnumeric(freq))
        freq = num2str(freq);
    end
    filename = sprintf('%sHZ.mat',freq);
    load(filename, 'compPres', 'd');
    air_mics = find(d>depth);
    amplitude=abs(compPres(air_mics));%[amp1,amp2];
    frequency = freqs(i);%(freq1+freq2)/2;

    %Initial parameter estimates
    %Estimate beta to be expected beta in air
    %Estimate incident pressure as maximum pressure in the tube
    beta = 2*pi*frequency/c_air;
    abs_Pi = max(amplitude);
    %Array for theta between pi/50 and 2pi
    d_theta = pi/50;
```

```

theta = d_theta:d_theta:2*pi;
%Array for incident pressure between 20% and 120% of estimate
d_Pi = abs_Pi/75;
Pi = 0.2*abs_Pi:d_Pi:1.2*abs_Pi-d_Pi;
%Array for reflection coefficient magnitude, between 0 and 1
d_gamma = 0.01;
gamma = d_gamma:d_gamma:1;
%Iterate over all the possible gamma, beta, Pi combinations
%Use only the mics in the air amplitude(1:last_mic)
%Find the current error, compare with previous smallest error
%Update parameters if the current error is lower
MMSE = [sum(amplitude.^2)];
for i_gamma = 1:length(gamma)
    for i_Pi = 1:length(Pi)
        for i_theta = 1:length(theta)
            est = Pi(i_Pi)*sqrt(1+gamma(i_gamma)^2+2*gamma(i_gamma)*...
                cos(2*beta*(d(air_mics)-depth)-theta(i_theta)));
            error = amplitude - est;
            MSE = sum(error.^2);
            if(MSE < MMSE)
                MMSE = MSE;
                best_Pi = Pi(i_Pi);
                best_gamma =gamma(i_gamma);
                best_theta = theta(i_theta);
            end
        end
    end
end;
%Store the best results, and write to the command line
MMSE = MMSE;
Pi = best_Pi;
gamma = best_gamma;
theta = best_theta ;
%Best fit curve
p = Pi*sqrt(1+gamma^2+2*gamma*cos(2*beta*(tube_axis-depth)-theta));
%Derive the SWR, complex gamma, impedance relative to the air
SWR = (1+abs(gamma))/(1-abs(gamma));
gamma_i = gamma*exp(sqrt(-1)*theta);
Z_R = (1+gamma_i)/(1-gamma_i);
%Plot results and title graph

plot(tube_axis,p)
hold;plot(d(air_mics),amplitude,'ro');
xlabel('Distance from bottom plate (m)');
ylabel('Pressure (Pa)');
xlim([0 7.25]);
ylim([0 ceil(max(amplitude+amplitude/10))]);
title(sprintf('%s\n%s%0.4g%s%0.3g%s%0.3g%s%0.3g + j%0.3g',...
    graphtitle,'f = ', frequency,' Hz, |\Gamma| = ',...
    gamma,' \Theta = ',theta,' SWR = ',SWR,' Z_L/Z_0 = ',...
    real(Z_R),imag(Z_R)}))
%cd(root2);cd('..');
%Save the results
saveas(gcf,[num2str(freq) 'HZ_SWR.png']);
save(sprintf('parameters_%sHz',freq), 'tube_axis', 'p', 'amplitude',...
    'Pi', 'gamma', 'theta', 'frequency', 'Z_R', 'SWR');
hold;

```

```
    clf;  
end
```

D.2 getCompPres.m

```
function[mags, phases, d]=getCompPres (uproot, loroot, upchans, upports, lochans, lop
orts, f)
%wave_length = 50050;
ports=[upports loports];

portHeights=[7.05, 6.85, 6.65, 6.4588, 6.257, 6.054, 5.853, 5.651, 5.448, 5.248, ...
    5.047, 4.845, 4.645, 4.441, 4.238, 4.038, 3.84, 3.64, 3.441, 3.237, 3.034, ...
    2.829, 2.629, 2.425, 2.223, 2.023, 1.818, 1.616, 1.414, 1.212, 1.012, ...
    0.811, 0.611, 0.41, 0.2 0];
%mags=zeros(length(ports), length(f));
%phases=zeros(length(ports), length(f));
len_up = length(upchans);
len_low = length(lochans);

cd([uproot '\PRECAL'])
for i=1:len_up
    chan=['CH' num2str(upchans(i))];
    cd(chan);
    load sensDat;
    sens(i)=sensDat;
    cd ..;
end

cd([loroot '\PRECAL'])
for i=1:len_low
    chan=['CH' num2str(lochans(i))];
    cd(chan);
    load sensDat;
    sens2(i)=sensDat;
    cd ..;
end

for fn=1:length(f)
    display(f(fn))

    cd([uproot '\' num2str(f(fn)) 'HZ'])
    for i=1:len_up
        chan=['CH' num2str(upchans(i))];
        cd(chan);
        load eventWaveform;
        load eventHeader;
        bin = f(fn)*length(waveform)/samplingRate;
        calwave=waveform./sens(i);
        fcal = fft(calwave);
        [a b]=max(abs(fcal(round(bin-bin*.1):round(bin+bin*.1)))));
        cP(i,fn) = fcal(round(bin-bin*.1)+b-1)/length(waveform);
        bin_num(i) = round(bin-bin*.1)+b-1;
        freq(i) = bin_num(i)*samplingRate/length(waveform);
        cd ..;
    end

    tempnum=length(upchans);

    cd([loroot '\' num2str(f(fn)) 'HZ'])
```

```

for i=1:len_low
    chan=['CH' num2str(lochans(i))];
    cd(chan);
    load eventWaveform;
    load eventHeader;
    bin = f(fn)*length(waveform)/samplingRate;
    calwave=waveform./sens2(i);
    fcal = fft(calwave);
    [a b]=max(abs(fcal(round(bin-bin*.1):round(bin+bin*.1))));
    cP(i+tempnum,fn) = fcal(round(bin-bin*.1)+b-1)/length(waveform);
    bin_num(i+tempnum) = round(bin-bin*.1)+b-1;
    freq(i+tempnum) = bin_num(i+tempnum)*samplingRate/length(waveform);
    cd ..;
end
for j=2:length(freq)
    if abs(freq(1) - freq(j)) > .02
        display(sprintf('Warning: Channel 1 frequency bin (%f Hz)'...
            'does not match Channel %d frequency bin (%f Hz)', freq(1),...
            j, freq(j)));
    end
end

dirname=[num2str(f(fn)) 'HZ'];
d=portHeights(ports);
cd([loroot '\..\'])
compPres = cP(:,fn);
save(dirname, 'd', 'compPres', 'bin_num', 'freq');
%figure
%subplot(2,1,1)
%plot(d,abs(compPres),'o-');
%title([num2str(f(fn)) ' Hz']);
%subplot(2,1,2)
%plot(d,angle(compPres),'o-');
%clear calwaves Calwaves
end
mags = abs(cP);
phases = angle(cP);

```

D.3 getAlpha_zero.m

```
function [abest Pin_best lbest]=getAlpha_zero(d,P,fc,d_medium)
%%%%%%%%%%%%%%%%%%%%%%%%%%%%%%%%%%%%%%%%%%%%%%%%%%%%%%%%%%%%%%%%%%%%%%%%
%Description: Curve-fitting algorithm for obtaining attenuation parameters
%            of porous medium in BYT using transmission line Equation for standing
%            waves in lossy lines .
%Input: d= distances from bottom of BYT
%       p= complex pressures for a particular single freq test
%       fc= frequency of the test
%       d_medium= depth of porous medium
%Output: abest= attenuation constant
%        Pin_best= value of incident pressure at the bottom of BYT
%        lbest= wavelength within medium
%*****

%set range of values for alpha and lambda to be tested
alpharange=.4:0.01:.6;
lambdarange=2:0.1:6;

P_material = P(d < d_medium);
d_material = d(d < d_medium);

no_mic_zero = sum(d == 0) == 0;
if no_mic_zero
    [a b] = min(d_material);
    real_max = real(P_material(b));
    imag_max = imag(P_material(b));

    if 0 % manual toggle: set to 1 to use the preset ranges for Pr and Pi
        % set to 0 to use the manually chosen values below

        if real_max < 0
            Pr_range = real_max*2:.1:real_max*.5;
        else
            Pr_range = real_max*.5:.1:real_max*2;
        end
        if imag_max < 0
            Pi_range = real_max*2:.1:real_max*.5;
        else
            Pi_range = real_max*.5:.1:real_max*2;
        end

        %manually chosen values for Pi and Pr to be tested
        else
            Pi_range = -5:.2:5;
            Pr_range = -5:.2:5;
        end
        %real_max = max(abs(real(P_material)));
        %imag_max = max(abs(imag(P_material)));
        disp('There is no mic at x=0, estimating Pin');
    else
        P_zero = P(d == 0);
        phase_zero = angle(P_zero);
        P = (P*exp(-phase_zero*(1i)));
        P_material = P(d < d_medium);
    end
end
```

```

    Pin = P_material(d_material == 0)/2;
end

%numdata=length(d_material);
Gr=1; %Refl coeff
maxerr=inf;

for lambda=lambdarange
    for alpha=alpharange
        %Estimate Pin assuming the last data point is the port
        %just above the bottom of BYT
        %*****Check if should be real(...) or abs(...)*****

        if(no_mic_zero) %no mic at x=0
            %error('There is no microphone at x=0')

            for Pin_r = Pr_range
                for Pin_i = Pi_range
                    Pin = Pin_r + li*Pin_i;
                    errors = get_errors(d_material, P_material, Pin,...
                        alpha, lambda, Gr);
                    mse=mean(errors);

                    if mse<maxerr
                        Pin_best=Pin;
                        maxerr=mse;
                        abest=alpha;
                        %Pbest=Ptest;
                        lbest=lambda;
                    end
                end
            end
        else
            %zero_mic = find(d == 0);

            errors = get_errors(d_material, P_material, Pin, alpha,...
                lambda, Gr);

            mse=mean(errors);

            if mse<maxerr
                Pin_best=Pin;
                maxerr=mse;
                abest=alpha;
                %Pbest=Ptest;
                lbest=lambda;
            end
        end
    end
end
if no_mic_zero
    phase_zero = angle(Pin_best);
    P = (P*exp(-phase_zero*(li)));
    disp(sprintf('Real(Pin) = %f, Imag(Pin) = %f',real(Pin_best),...

```

```

        imag(Pin_best));
    Pin_best = (Pin_best*exp(-phase_zero*(1i)));

    %P_material = P(d < d_medium);
end
plot_standing_wave(Pin_best, abest, lbest,d,P,d_medium,Gr,fc);
return

function plot_standing_wave(Pin_best,abest,lbest,d,P,d_medium,Gr,fc)
%plot the real part, imaginary part, absolute value,
%and phase of the standing wave

ddisp=0:0.01:d_medium;
Pbest2=greens_function(Pin_best, ddisp, abest, lbest, Gr);
figure
title_str = sprintf('%1.2f m Large Pea Gravel - %1.2f Hz\n\\alpha'...
' = %1.2f, \\lambda = %1.2f, P_{in} = %1.2f\nReal Part', d_medium, fc,...
abest, lbest, Pin_best);
%title(title_str);

subplot(4,1,1)
hold on
%title('Real Part')
title(title_str)
plot(d,real(P),'o')
plot(ddisp,real(Pbest2),'r')
plot([d_medium; d_medium],ylim,'k--')
xlabel('height (m)');
ylabel('pressure (Pa)');

subplot(4,1,2)
hold on
title('Imaginary Part')
plot(d,imag(P),'o')
plot(ddisp,imag(Pbest2),'r')
plot([d_medium; d_medium],ylim,'k--')
xlabel('height (m)');
ylabel('pressure (Pa)');

subplot(4,1,3)
hold on
title('Magnitude')
%title(title_str)
plot(d,abs(P),'o')
plot(ddisp,abs(Pbest2),'r')
plot([d_medium; d_medium],ylim,'k--')
xlabel('height (m)');
ylabel('pressure (Pa)');

subplot(4,1,4)
hold on
title('Phase')
plot(d,angle(P),'o')
plot(ddisp,angle(Pbest2),'r')
plot([d_medium; d_medium],ylim,'k--')

```

```

xlabel('height (m)');
ylabel('phase (rad)');

filestr = sprintf('%.fHZ_inMedium',fc);
print('-dpng', filestr);

return

function [errors] = get_errors(d, P, Pin, alpha, lambda,Gr)
%find the mean square error from a particular iteration
numdata = length(d);
Ptest = zeros(numdata,1);
errors = zeros(numdata,1);
for m=1:numdata
    Ptest(m)= greens_function(Pin, d(m), alpha, lambda, Gr);

    errors(m)=(P(m)-Ptest(m)).*conj(P(m)-Ptest(m));
end

return

function [pressures] = greens_function(Pin, d, alpha, lambda, Gr)
pressures = Pin*(exp(d*(alpha+1i*(2*pi/lambda)))+...
    Gr*exp(-d*(alpha+1i*(2*pi/lambda))));

```

D.4 run_getAlpha_zero.m

```
function [a l] = run_getAlpha_zero(freqs, d_medium)
%program to call getAlpha_zero for several data sets in succession

a = zeros(length(freqs),1);
l = zeros(length(freqs),1);
x = 1;
for j=freqs
    filestr = sprintf('%dHZ.mat',j);
    load(filestr);
    compPres(d==0) = -compPres(d==0);

    [a(x) p l(x)] = getAlpha_zero(d,compPres,freq(1),d_medium);
    x=x+1;
end
```